CANCER

Interaction between NF-κB and PLAC8 impairs autophagy providing a survival advantage to prostate cells transformed by cadmium

Vaibhav Shukla[1]†, Ashish Tyagi[1]†, Balaji Chandrasekaran[1], Bhawna Tyagi[1], Balpreet Singh[1], Thulasidharan Nair Devanarayanan[1], Venkatesh Kolluru[2], Murali K. Ankem[2], Chendil Damodaran[1]*

Prostate cancer risk is influenced by various factors, including exposure to heavy metals like cadmium (Cd). The study reveals that the autophagy-regulating gene PLAC8 (placenta-specific 8) is significantly involved in Cd-induced prostate carcinogenesis, and NF-κB acts as the upstream transcriptional activator of PLAC8, which then selectively up-regulates BCL-xL, providing a survival advantage to Cd-transformed cells. NF-κB activation stabilizes PLAC8 in the cytosol, disrupting autophagy by allowing PLAC8 to colocalize with LC3B instead of LAMP1. Silencing NF-κB down-regulates PLAC8 and its survival function while inhibiting NF-κB or PLAC8, which restores autophagy and decreases tumor growth in xenograft models. In addition, targeting BCL-xL confirmed this signaling pathway. The findings suggest that sustained NF-κB activation regulates PLAC8 and highlights the NF-κB–PLAC8–BCL-xL axis as a potential target for early detection and therapies in metal-induced prostate cancer.

INTRODUCTION

Macroautophagy (often referred to as autophagy) is an intracellular degradation system, which is initiated when isolation membranes first appear to engulf cytoplasmic components, expanding to form closed, double-membrane autophagosomes. Once formed, autophagosomes fuse with lysosomes, releasing acidic proteases that degrade the engulfed cytoplasmic components. During this process, a cytosolic form of microtubule-associated protein light chain 3 (LC3a) transforms into phosphatidylethanolamine-conjugated LC3 (LC3b). LC3b then fuses with LAMP1, a lysosomes marker, and forms an autolysosome which is essential for degradation of cellular components (*1*, *2*). When the conversion of LC3a to LC3b is hindered, or if LAMP-1 fails to fuse with LC3b, then autophagy flux is impaired, and autophagy may be considered defective (*3*). This can lead to the accumulation of autophagosomes and ineffective degradation of their contents (*4*). The accumulation of damaged proteins and organelles also contributes to oncogenesis by promoting genomic instability and disrupting cellular homeostasis (*5*) and is now recognized as a critical contributing factor in the development and progression of prostate cancer (*6*).

Prostate cancer can arise from a combination of genetic and environmental factors (*7*). Notably, there is an evident link between heavy metal exposure, whether through the environment or occupation, to the incidence of prostate cancer (*8*, *9*), and the aggressiveness of the disease (*10*). Cadmium (Cd) is one such heavy metal (*11*) that is increasingly used in many applications (*12*). Previous work demonstrated that chronic exposure (12 months) to Cd (10 μM) resulted in the transformation of human normal prostate epithelial cells (RWPE-1) to a malignant phenotype [Cd-transformed prostate epithelial (CTPE) cells]. Furthermore, we demonstrated that Cd-induced reactive oxygen species may be implicated in the impairment of autophagy, thereby facilitating the transformation of normal prostate epithelial cells (*6*). Several transcription factors are known to regulate the autophagic process and contribute to carcinogenesis and metastasis, including placental-specific 8 (PLAC8) (*13*, *14*). Our findings suggest that a progressive increase in PLAC8 expression is associated with Cd-induced prostate carcinogenesis, observed in vitro and in xeno-transplanted mice (*15*). However, the molecular signaling mechanisms underlying PLAC8 function and its role in regulating autophagy in prostate cancer remain to be elucidated.

Cd exposure also causes prostate cancer by activating cellular proliferation, differentiation, apoptosis, and/or angiogenesis pathways; inhibiting DNA repair; and inducing oxidative stress (*16*, *17*). Oxidative stress and inflammation activate nuclear factor κB (NF-κB) or p65, a molecule that plays a vital role in cell survival, proliferation, and invasion (*18*). NF-κB is thought to transactivate *PLAC8* expression in colon (*19*) and breast cancer (*20*), so we hypothesized that Cd-induced oxidative stress–mediated NF-κB activation may regulate PLAC8, which could be a mechanism for prostate carcinogenesis. In this study, we demonstrate that the activation of NF-κB is a key factor driver that regulates PLAC8 function during Cd-induced cell transformation. NF-κB stabilizes PLAC8, which, in turn, prevents the fusion (or colocalization) of autophagosomes and lysosomes thus facilitating cell proliferation and contributes to malignancy. The coordinated actions of NF-κB and PLAC8 enable the precise regulation of the survival gene BCL-xL. This molecular regulatory network helps cells maintain viability and resist apoptosis, thereby promoting survival in conditions that would typically lead to cell death.

RESULTS

PLAC8 colocalizes with LC3B and drives defective autophagy

Cd-induced transformation of prostate epithelial cells triggered PLAC8 expression. There was also a concurrent increase in the expression of the autophagy-regulated genes LC3B and LAMP1 (Fig. 1A and fig. S1, A and B). The induction of LC3B and LAMP1 expression was expected to enhance the fusion of autophagosomes and lysosomes, resulting in the formation of autolysosomes in a

[1]College of Pharmacy, Texas A&M University, College Station, TX, USA. [2]Department of Urology, University of Louisville, Louisville, KY, USA.
*Corresponding author. Email: chendamodar@tamu.edu
†These authors contributed equally to this work.

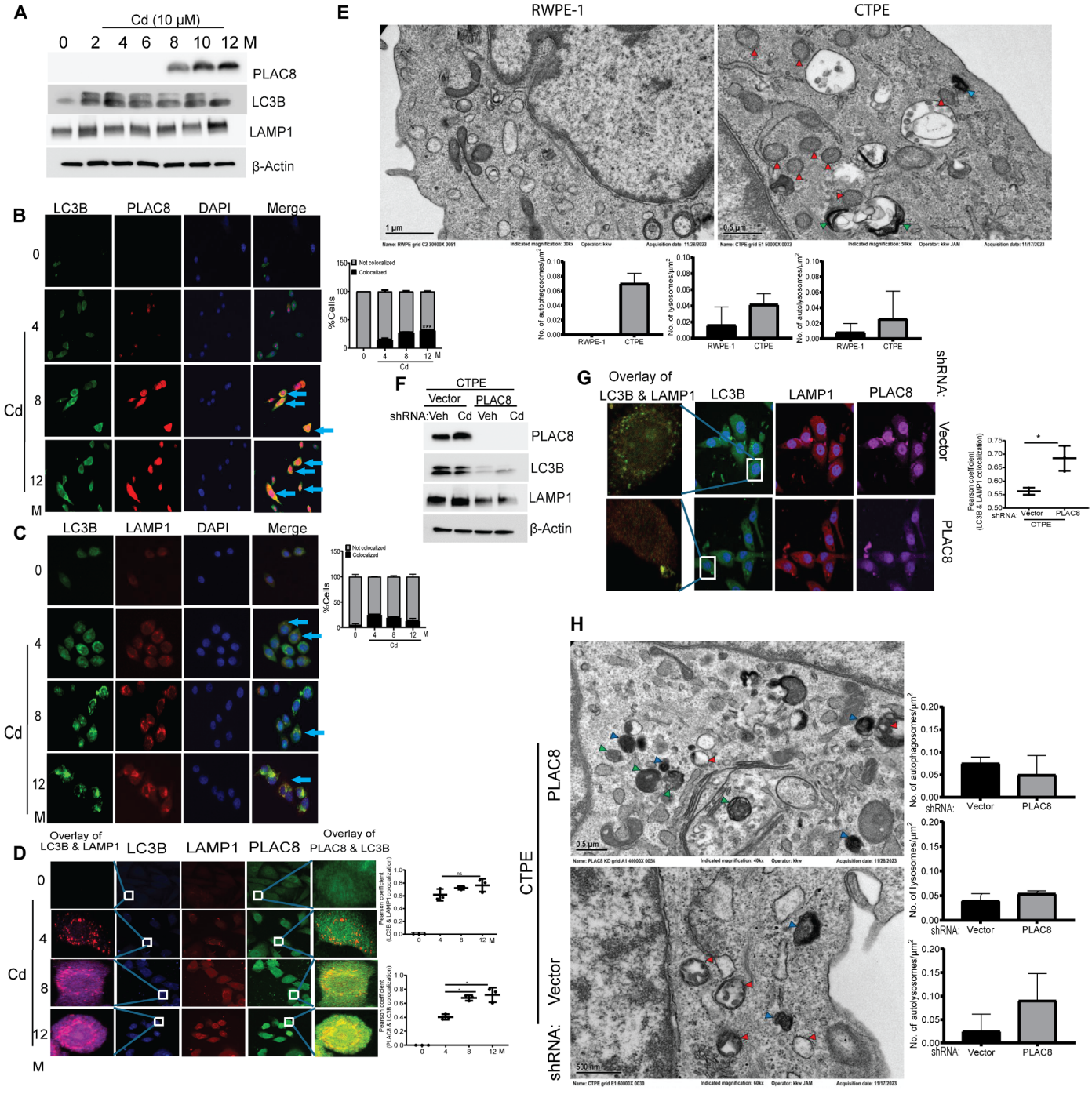

Fig. 1. Induction of PLAC8 leads to defective autophagy and transformation in prostate epithelial cells exposed to Cd. (**A**) Western blot analysis confirming induction of autophagy signaling following chronic exposure to Cd in prostate epithelial cells. (**B**) Immunofluorescence of RWPE-1 and Cd-transforming cells shows an increase in percentage of cells with LC3B and PLAC8 fusion. (**C**) Immunofluorescence of RWPE-1 and Cd-transforming cells shows a decrease in percentage of cells with LC3B and LAMP-1fusion. (**D**) Immunofluorescence staining and the colocalization analysis of LC3B with LAMP1 and PLAC8 were assessed using Pearson coefficient. (**E**) Representative TEM images illustrating the fusion of autophagosomes and lysosomes in RWPE-1 and CTPE cells, along with quantification of autophagosomes, lysosomes, and autolysosomes per square micrometer. (**F**) The expression levels of PLAC8, LAMP1, and LC3B were determined by Western blot analysis in shRNA-PLAC8–transfected cells, both in the presence and absence of Cd. Veh, vehicle. (**G**) Immunofluorescence staining and colocalization analysis of LC3B and LAMP1 fusion with increased Pearson coefficient in sh-PLAC8 CTPE cells. (**H**) Representative TEM images showing fusion of autophagosomes and lysosomes in shRNA PLAC8-transfected CTPE cells compared to vector alone, along with the quantification of autophagosomes, lysosomes, and autolysosomes per square micrometer. Arrowheads indicate the following: lysosomes (blue), autophagic vacuoles (red), and autolysosomes (green). All error bars represent means ± SD. Statistical significance: $^*P < 0.05$; ns, not significant.

classical autophagy process (*21*). However, our findings revealed that LC3B colocalizes with PLAC8 rather than LAMP1, resulting in a gradual decline in the fusion of LC3B and LAMP1 during the transformation process (Fig. 1, B and C). To investigate the inhibition of autophagosome and lysosome fusion in transforming cells, we measured the fusion rates of LC3B with LAMP1 and LC3B with PLAC8 in individual cells using multicolor immunofluorescence and confocal microscopy. We observed LC3B and LAMP1 fusion as early as 4 months, but no significant increase occurred during the 8th and 12th months of transformation. In contrast, colocalization between LC3B and PLAC8 showed a steady increase throughout the successive stages of transformation, suggesting that PLAC8 may replace LAMP1 in fusion with LC3B (Fig. 1D). This shift resulted in the inhibition of autolysosome formation, which we confirmed through transmission electron microscopy (TEM). We found more autophagosomes but not autolysosomes in CTPE cells (Fig. 1E).

To elucidate how PLAC8 regulates autophagy, we transfected Cd-transformed RWPE-1 (CTPE) cells with either scrambled/control short hairpin RNA (shRNA) or *PLAC8*-shRNA and subsequently treated them with an acute Cd dose (10 μM). Inhibition of PLAC8 resulted in impaired colony formation (fig. S1C). As expected, the expression levels of autophagy-related genes, LC3B and LAMP1, increased following acute exposure to Cd. Conversely, in PLAC8 knockdown CTPE cells, Cd exposure did not restore the expression of LC3B and LAMP1 which had decreased because of PLAC8 knockdown (Fig. 1F and fig. S1D). Reduced expression of PLAC8 notably increased the colocalization of LC3B and LAMP1, leading to an increased number of autolysosomes in Cd-treated cells (Fig. 1, G and H). This finding suggests that PLAC8 inhibits the formation of the LC3B-LAMP1 complex and plays a crucial role in defective autophagy, which contributes to the Cd-induced transformation of human prostate epithelial cells.

Inhibiting PLAC8 suppresses tumor burden

To explore whether suppressing *PLAC8* can inhibit tumor growth in vivo, we generated CTPE cells that stably expressed sh-PLAC8 or an empty vector and subcutaneously transplanted them into nude mice. After 4 weeks, tumors from the sh-PLAC8 group were significantly smaller than those from the vector control group (Fig. 2A). The silenced PLAC8 was confirmed by Western blot analysis in CTPE transfectants (Fig. 2A). Tumors with sh-PLAC8 knockdown tumors also had reduced PLAC8, LC3B, and LAMP1 expression and reduced cell proliferation marker (Ki67 expression; Fig. 2B). Together, these in vivo results demonstrated that lower PLAC8 expression can inhibit CTPE tumor growth. By performing RNA sequencing (RNA-seq), we assessed whether the significant inhibition of tumor burden was a direct consequence of PLAC8 knockdown. We identified 1610 down-regulated genes [$\log_2$ fold change (FC) ≤ -1, $P \leq 0.05$] and 339 up-regulated genes ($\log_2$FC ≥ 1, $P \leq 0.05$) (Fig. 2C). Gene set enrichment analysis (GSEA) indicated that knocking down PLAC8 attenuated lysosomal function, prostate cancer, cancer pathways, androgen response, and tumor necrosis factor–α (TNF-α) signaling via NF-κB pathways (Fig. 2D, fig. S2A, and table S2). Knocking down PLAC8 also decreased the expression of known prostate cancer driver genes, including *SLC17A5*, *IFIH1*, *LIFR*, *PGM3*, *CASP8*, *FZD5*, and *ITGAV* (fig. S2B). The findings support the idea that PLAC8 contributes to impaired autophagy and promotes factors that lead to prostate carcinogenesis.

p65 regulates PLAC8 and induces key molecular changes

Since knocking down PLAC8 down-regulated the NF-κB signaling pathway (Fig. 2D), we investigated the role of p65 in transforming cells. After exposing RWPE-1 cells to Cd for over a year, we observed an increase in p65 expression beginning at 4 months, peaking at 12 months (Fig. 2E and fig. S3, A and B). Typically, transcription factors, including p65, are localized in the cytoplasm and translocate to the nucleus upon activation (*22*). Therefore, we conducted an NF-κB activation assay, which revealed that NF-κB activation and nuclear translocation increased during the Cd-induced transformation of RWPE-1 cells (Fig. 2, F and G) starting from the fourth month, before the increase in PLAC8 expression. This suggests that the induction of p65 activation may influence PLAC8 expression.

To test this hypothesis, we first identified two p65 binding sites within the PLAC8 promoter (Fig. 2H, top). We then mutated both binding sites together and transfected RWPE-1 and CTPE cells with luciferase plasmids containing wild-type or mutant PLAC8 promoters. After transfection, we treated the cells with lipopolysaccharide (LPS) to induce NF-κB activation.

In CTPE cells with the wild-type PLAC8 promoter, LPS treatment significantly increased luciferase activity by 1.5-fold ($P < 0.05$) compared to vehicle control. In contrast, luciferase activity in CTPE cells containing the mutant PLAC8 promoter decreased, and neither LPS nor Cd treatment restored NF-κB activity in these cells (Fig. 2H). As expected, the increase in PLAC8 promoter activity in RWPE-1 cells was insignificant (fig. S3C). A chromatin immunoprecipitation–quantitative polymerase chain reaction (ChIP-qPCR) assay also confirmed that p65 binding to the PLAC8 promoter was higher in CTPE cells than in RWPE-1 cells (Fig. 2I).

This study confirms the interaction between NF-κB and PLAC8 in the nucleus, but the replacement of LAMP1 with PLAC8 occurs in the cytosol. So, we examined whether NF-κB plays a role in the sustained up-regulation of PLAC8 protein in the cytosol by investigating the protein-protein interaction between NF-κB and PLAC8. Immunoprecipitation experiments using a p65 antibody demonstrated direct interaction between p65 and PLAC8 in CTPE cells (Fig. 3A). Treatment with cycloheximide (CHX) stabilized PLAC8 expression in control cells; however, it failed to prevent the degradation of PLAC8 in p65 knockdown cells (Fig. 3B and fig. S3D). These findings suggest that p65 functions as both a scaffold and a transcriptional cofactor in promoting PLAC8 expression. Notably, both p65 and PLAC8 proteins colocalized (Fig. 3C), and a number of cells exhibiting colocalization have increased during the transformation (Fig. 3D), providing direct evidence of their involvement in Cd-induced transformation. In addition, these results align with previous observations that PLAC8 replaces LC3B in the cytoplasm, inhibiting normal autophagy while still bestowing survival characteristics to transformed cells.

We overexpressed p65 in RWPE-1 cells, which slightly increased PLAC8 expression (Fig. 3E and fig. S3E). In contrast, knocking down p65 in CTPE cells resulted in down-regulation of PLAC8, LC3B, and LAMP1 expressions. Notably, acute exposure to 10 μM Cd did not restore the expression of these important autophagy-related genes (Fig. 3F and fig. S3F). In addition, p65 knockdown in CTPE cells increased the colocalization of LC3B and LAMP1 (Fig. 3G). This phenomenon may be attributed to decreased PLAC8 levels (Fig. 3F), allowing for greater availability of free LC3B to bind with LAMP1. The fusion of LC3B and LAMP1 is a crucial step in autophagy, as it promotes the formation of autolysosomes and

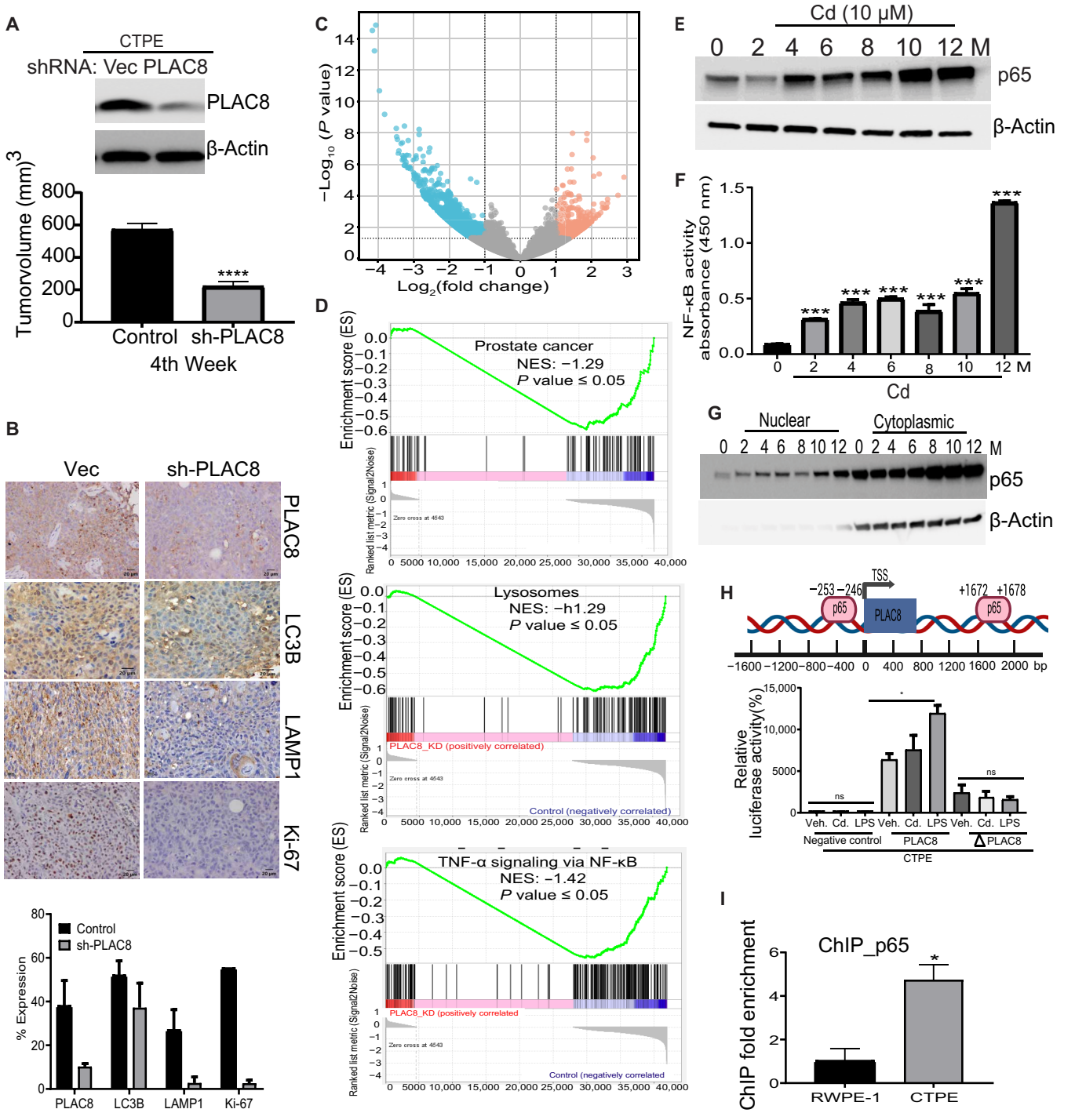

Fig. 2. Knocking down PLAC8 expression inhibits Cd-induced tumor growth in xenotransplanted mice. (**A**) In CTPE cells, silencing PLAC8 expression reduced tumor formation in the xenotransplantation model. (**B**) Immunohistochemistry (IHC) of tumor tissues analyzed for Ki-67, PLAC8, LC3b, and LAMP1 expression. (**C**) A volcano plot analysis displayed the differential expression of genes in sh-PLAC8 tumors compared to the control group. (**D**) GSEA identified pathways associated with prostate cancer, lysosomal functions, and NF-κB–mediated TNF-α signaling in PLAC8-knockdown (PLAC8_KD) tumors compared to the vector control. (**E**) Cd-transforming cells showed a time-dependent induction of p65 expression (**F**) and NF-κB activation was observed. (**G**) Both cytosolic and nuclear expression of p65 were noted during the transformation of Cd-exposed RWPE-1 cells. (**H**) p65 binding sites on the PLAC8 promoter were identified and validated by comparing luciferase activity in wild-type and mutated (Δ) sites, transcription start sites (TSS) and (**I**) ChIP-qPCR was performed in CTPE cells. All error bars represent means ± SD, with statistical significance indicated as $*P < 0.05$, $***P < 0.001$; ns, not significant. NES, normalized enrichment score.

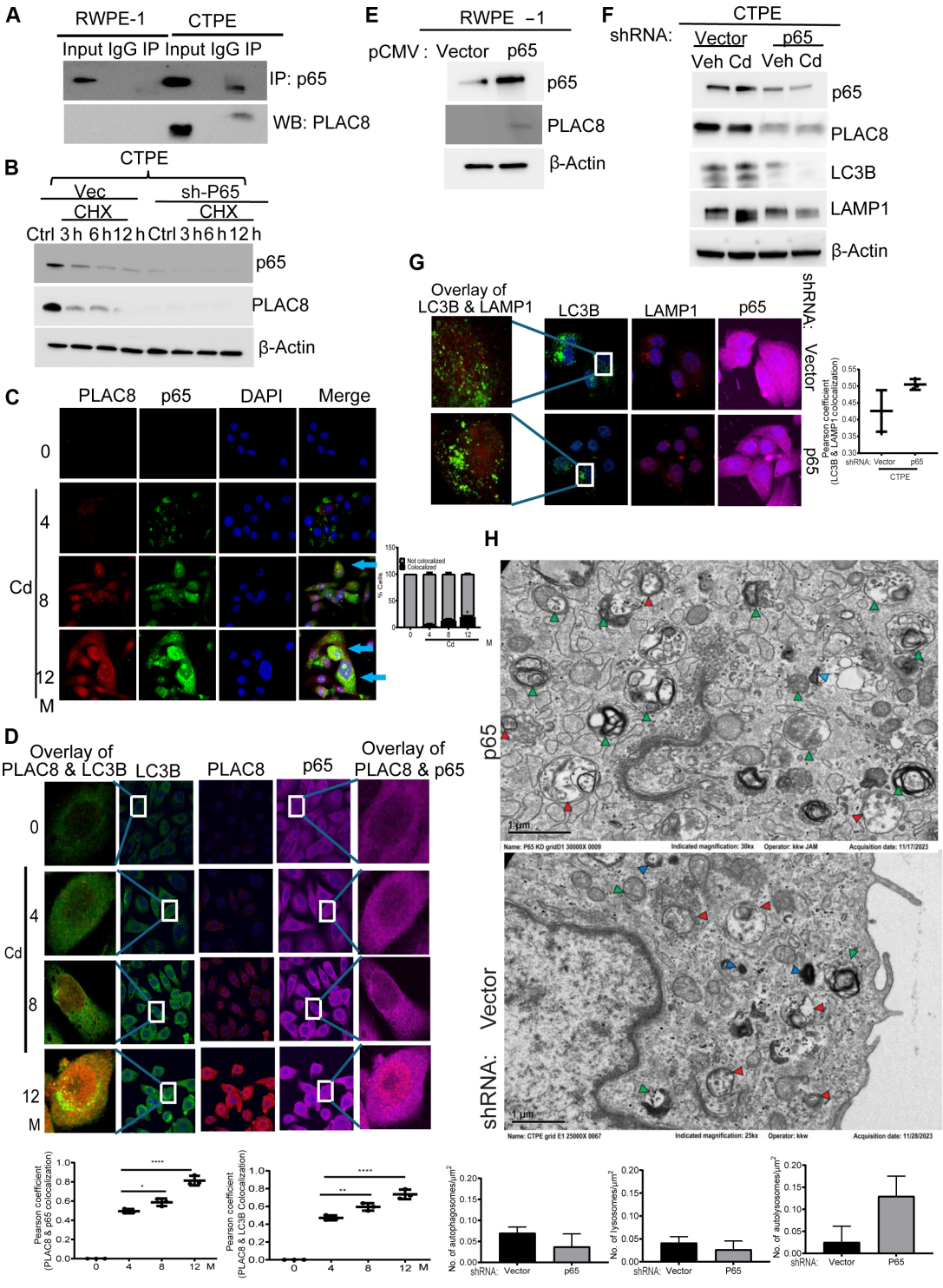

Fig. 3. The interaction between PLAC8 and NF-κB during the transformation of prostate epithelial cells. (**A**) The interaction between p65 and PLAC8 is confirmed by immunoprecipitation (IP) analysis. IgG, immunoglobulin G. (**B**) CHX was used to inhibit protein synthesis in vector alone and sh-p65 cells, and Western blot (WB) analysis was performed to show that p65 is necessary to stabilize PLAC8 in CTPE cells. h, hours. (**C**) Immunofluorescence of RWPE-1 and Cd-transforming cells shows an increase in percentage of cells with PLAC8 and p65 colocalization. (**D**) Immunofluorescence staining and the colocalization analysis of p65 and PLAC8 were assessed using Pearson coefficient. (**E**) Ectopic expression of p65 increases PLAC8 expression in RWPE-1 cells. (**F**) The expression levels of p65, PLAC8, LAMP1, and LC3B were determined by Western blot analysis in sh-p65–transfected cells, both in the presence and absence of Cd. (**G**) Immunofluorescence staining and colocalization analysis of LC3B and LAMP1 fusion with increased Pearson coefficient in sh-p65 CTPE cells. (**H**) Representative TEM images showing fusion of autophagosomes and lysosomes in sh-p65–transfected CTPE cells compared to vector alone, along with the quantification of autophagosomes, lysosomes, and autolysosomes per square micrometer. Arrowheads indicate lysosomes (in blue), autophagic vacuoles (in red), and autolysosomes (in green). All error bars represent means ± SD. Statistical significance is indicated as $*P < 0.05$, $**P < 0.01$, and $****P < 0.0001$.

decreases cell viability. TEM confirmed that cells with p65 knockdown contained more autolysosomes than control cells (Fig. 3H). Furthermore, p65 knockdown decreased the proliferation of CTPE cells, and additional exposure to Cd further inhibited cell growth (fig. S4A). These findings suggest that the activation of p65, its subsequent translocation to the nucleus, and its interaction with PLAC8 are critical events that contribute to defective autophagy in transforming prostate epithelial cells.

p65 knockdown abrogates CTPE tumor growth

The stable knockdown of p65 in CTPE cells was confirmed across different clones, and following this confirmation, these cells were subcutaneously inoculated into nude mice (Fig. 4A, left). After 4 weeks, tumors in the sh-p65 group were significantly smaller than those in the corresponding vector control group (Fig. 4A, right). Differential gene expression analysis revealed that sh-p65 tumors had 68 activated genes and 86 repressed genes compared to the control tumors (Fig. 4B). Notably, pathways related to proteasomal degradation, autophagy, apoptosis, and unfolded protein response were positively enriched. In contrast, oxidative phosphorylation was negatively enriched (Fig. 4C, fig. S4B, and table S3). In contrast, PLAC8 knockdown down-regulated genes are associated with prostate cancer and lysosomal pathways (Fig. 2D). The p65 knockdown activated programmed cell death pathways, including autophagy and apoptosis. In addition, p65 knockdown decreased the expression of PLAC8, LC3B, and LAMP1 (Fig. 4, D and E), which aligns with the reduced cell proliferation and viability observed in the CTPE tumors. To confirm that the observed cell death was partially due to apoptosis, we stained the cells with annexin V–fluorescein isothiocyanate (FITC) and performed a fluorescence-activated cell sorting analysis. This analysis showed an elevated fraction of apoptotic cells (Fig. 5A). These results indicate that p65 activation is essential for the growth of Cd-transformed tumors and suggest that p65 knockdown could be a potential therapeutic strategy for inhibiting tumor growth.

PLAC8-dependent *BCL-xL* expression drives the survival of transformed cells

BCL-xL and BCL2 play crucial roles in regulating cell survival during carcinogenesis (*22*). We found that overexpressing PLAC8 substantially increased the levels of BCL-xL and decreased BCL2 (Fig. 5B and fig. S4C). In addition, up-regulation of BCL-xL was seen during the Cd-induced transformation process (Fig. 5C and fig. S4, D and E). These results suggest that BCL-xL may be the primary effector molecule responsible for the survival of RWPE-1 cells in response to chronic Cd exposure. Furthermore, knocking down BCL-xL resulted in decreased expression levels of p65 and PLAC8 (Fig. 5D and fig. S5A). Conversely, overexpression of BCL-xL was found to increase the levels of p65 and PLAC8 (Fig. 5E and fig. S5B). This suggests a feedback loop mechanism within the NF-κB (p65)–PLAC8–BCL-xL axis in Cd-transformed cells. In addition, knocking down BCL-xL in RWPE-1 cells that overexpress PLAC8 significantly reduced cell viability (fig. S5C).

To explore whether BCL-xL expression is influenced by p65 or PLAC8, we overexpressed p65 in PLAC8-knockdown CTPE cells and observed no change in BCL-xL levels (Fig. 5F). We also confirmed the interaction between p65 and BCL-xL in CTPE cells through immunoprecipitation (fig. S5D). Furthermore, a dual luciferase assay indicated that BCL-xL promoter activity was elevated in CTPE cells (Fig. 5G) and in RWPE-1 cells that overexpress PLAC8 (fig. S5E), these data suggest that NF-κB (p65) regulates PLAC8 and, indirectly, BCL-xL through PLAC8. This suggests a feedback loop mechanism within the NF-κB (p65)–PLAC8–BCL-xL axis in Cd-transformed cells, indicating that NF-κB contributes to PLAC8 expression, which, in turn, regulates BCL-xL and controls the survival of Cd-transformed cells.

BCL-xL inhibition reprograms cell death pathways

We next used pharmacological inhibitors and shRNA knockdown strategies to investigate the role of BCL-xL in Cd-induced tumor growth. A BCL-xL inhibitor (A-1331852) significantly slowed the growth rate of xenografted tumors (Fig. 6A), as did shRNA-mediated BCL-xL knockdown (Fig. 6B). The shBCL-xL tumors also exhibited reduced proliferation, as indicated by decreased Ki67 expression and lower levels of p65 and PLAC8 (Fig. 6C). BCL-xL xenograft tumors had 166 up-regulated genes and 256 down-regulated genes relative to tumors from the vector control (Fig. 6D), with positively enriched pathways related to the unfolded protein response, autophagy, and apoptosis and negatively enriched pathways related to matrix metalloproteinases and oxidative phosphorylation (Fig. 6E, fig. S5F, and table S4). These findings suggest an approach that by inhibiting p65/PLAC8/BCL-xL axis may achieve a similar outcome in terms of tumor reduction. This potential enhancement of cancer therapy is a promising area for future research and development.

p65 and PLAC8 expression in clinical prostate cancer specimens

To assess the clinical significance of p65, PLAC8, and BCL-xL in prostate cancer progression, we divided clinical prostate cancer specimens into "low" (≤39 ng/g dry weight) and "high" (≥40 ng/g dry weight) Cd content, as previously reported (*23*). Prostate cancer specimens with high Cd levels exhibited increased p65, PLAC8, and BCL-xL levels compared to specimens with low Cd content (Fig. 7A). Although the data suggest potential biological trends, this study's small sample size limited our ability to detect statistically significant differences. The induction of the p65/PLAC8/BCL-xL signaling axis in patients with high Cd levels aligns with our preclinical findings regarding CTPE cells.

We also analyzed prostate adenocarcinoma (PRAD) The Cancer Genome Atlas (TCGA) datasets to evaluate the expression of p65, PLAC8, and BCL-xL in clinical samples. Although Cd levels are not directly reported in the TCGA-PRAD datasets, they are linked to prostate cancer progression and metastasis. Therefore, we examined the expression of p65, PLAC8, and BCL-xL in metastatic PRAD samples according to the American Joint Committee on Cancer Neoplasm Clinical Distant Metastasis M Stage criteria. We focused on samples classified as stages 3b and 4 ($n = 39$) with high p65 expression and observed a significant up-regulation of PLAC8 and BCL-xL in these tumors compared to their nonmetastatic counterparts ($n = 52$; Fig. 7B and table S5). This suggests that the interaction between NF-κB (p65), PLAC8, and BCL-xL could be targeted to enhance therapeutic efficacy in Cd-induced prostate cancer.

DISCUSSION

Epidemiological evidence indicates that Cd is a contributing factor to prostate cancer (*24*), and rat models show that Cd exposure accelerates the malignant progression and distant metastases of

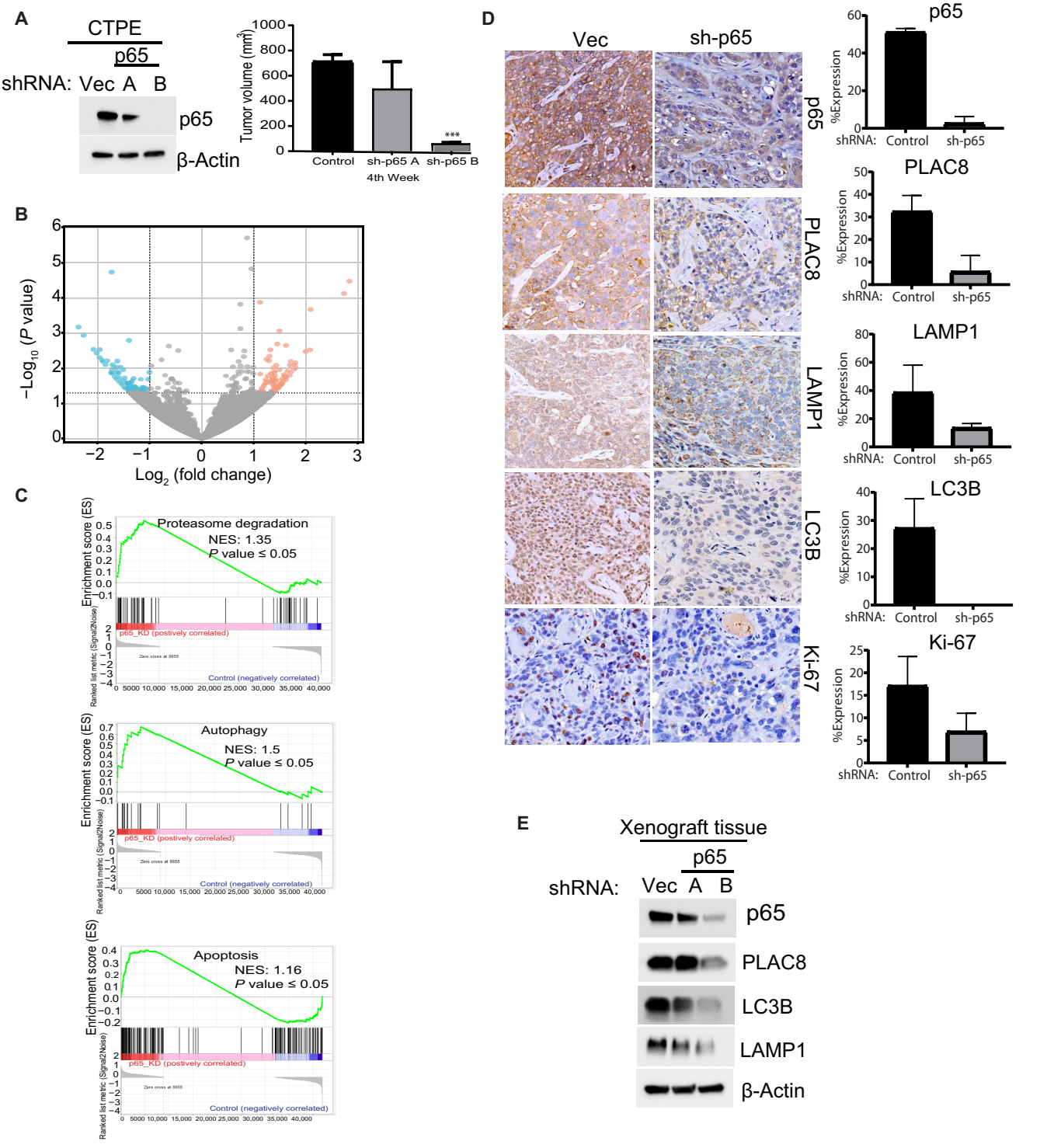

Fig. 4. Knockdown of p65 inhibits Cd-induced tumor growth in xenotransplanted mice. (**A**) Confirmation of stable p65 knockdown in CTPE cells via Western blot analysis (left side), with selected clones inoculated into nude mice to assess tumor inhibition. (**B**) A volcano plot analysis illustrates the differential expression of genes in sh-p65 tumors compared to the vehicle group. (**C**) GSEA plot shows pathways involved in proteasome degradation, autophagy, and apoptosis in sh-p65 tumors compared to the vector control. (**D**) IHC analysis was performed to determine the expressions of Ki-67, p65, PLAC8, LC3B, and LAMP1 in xenograft tumors from the vector and sh-p65 groups. (**E**) Protein expression levels of p65, PLAC8, LC3B, and LAMP1 in xenograft tumors from sh-p65 and vector-only groups. All error bars represent means ± SD, with ***$P < 0.001$.

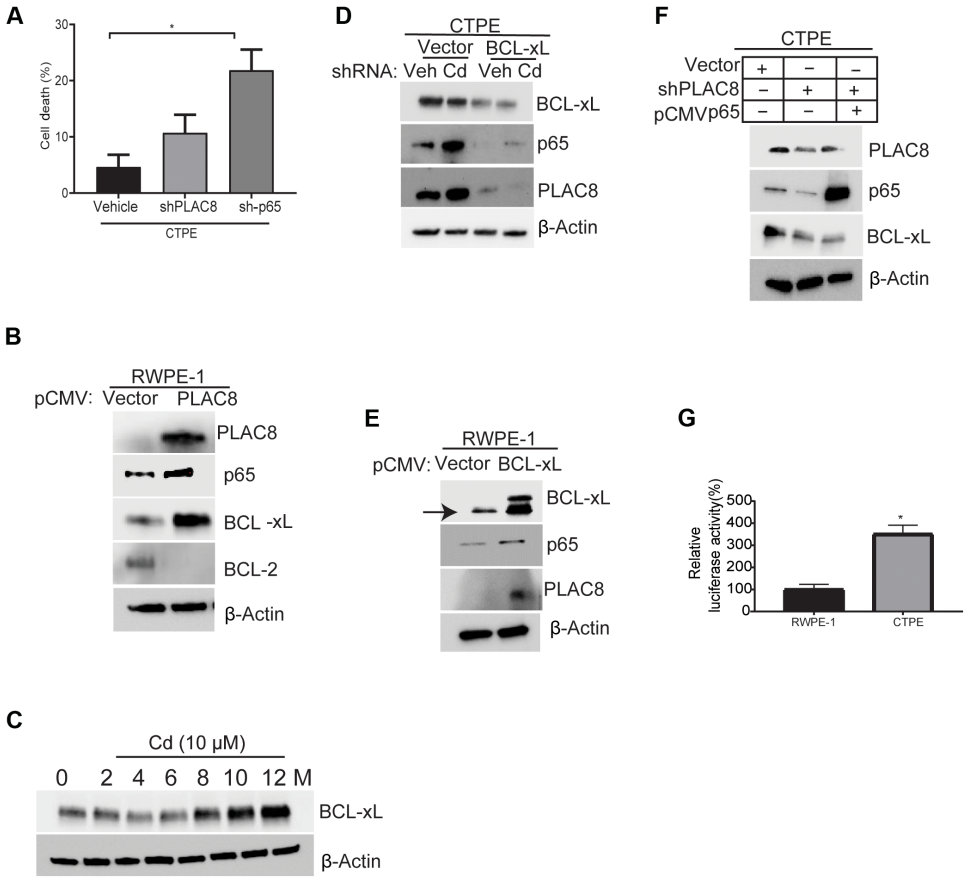

Fig. 5. BCL-xL plays a crucial role in the survival of transformed cells and is regulated by PLAC8. (**A**) Inhibiting the expression of p65 and PLAC8 enhances the induction of apoptosis in CTPE cells, confirmed by flow cytometry analysis of annexin V-FITC–stained apoptotic cells. (**B**) Ectopic expression of PLAC8 leads to increased levels of BCL-xL and p65 in RWPE-1 cells. (**C**) The expression of BCL-xL is observed at successive stages of Cd exposure during the transformation of RWPE-1 cells. (**D**) Silencing BCL-xL expression abolishes the PLAC8-mediated autophagy signaling in CTPE cells. (**E**) Ectopic expression of BCL-xL results in up-regulating PLAC8 and p65 in RWPE-1 cells. (**F**) In CTPE cells, cotransfection with sh-PLAC8 and the pCMV p65 overexpression plasmid demonstrated PLAC8, p65, and BCL-xL protein levels through Western blot analysis. (**G**) A luciferase assay showing increased BCL-xL promoter activity in CTPE cells compared to RWPE-1 cells. All error bars represent means ± SD, with statistical significance at $^*P < 0.05$.

tumors (*25*). Mechanistically, Cd exposure alters the prostatic lipid profile and metabolism, contributing to cellular damage (*26*). Short-term Cd exposure also triggers p53-dependent apoptosis in human prostate epithelial cells (*27*), whereas long-term or chronic exposure causes malignant transformation of nontumorigenic cells (*15*, *28*, *29*). Cd-transformed prostate cells can develop apoptotic resistance through BCL-2 overexpression (which hinders c-Jun N-terminal kinase signaling) (*30*) and a global down-regulation of caspase gene expression (*31*). Apoptosis-resistant cells had 2.5-fold more metallothionein compared to untreated controls, suggesting that Cd may preferentially select for apoptotic-defective cells, thus heightening the risk of tumor formation (*32*).

In our prior work, we showed that apoptosis resistance in chronically (12-month) exposed human prostate epithelial cells (RWPE-1 cells) due to PLAC8-induced defective autophagy (*15*). Apoptosis and autophagy collaborate to promote cell death; where one pathway is inhibited, the other can compensate to ensure effective cell elimination (*33*). PLAC8 localizes to the inner surface of the plasma membrane and (when activated) interacts with other cellular components to trigger autophagy, cell cycle arrest, and apoptosis (*14*). In the current study, chronic Cd exposure also increased LC3B and LAMP1 expression (key autophagy markers), along with PLAC8. LC3B is essential in the early stages of autophagosome formation where it mediates phagophore elongation, whereas LAMP1 is essential for the transition from early to late phagosomes and for the fusion of lysosomes with matured autophagosomes (*34*). Although we observed an increase in the expression of LC3B and LAMP1, there was no corresponding rise in the formation of autolysosomes. Studies have shown that the location of PLAC8 within lysosomes may affect the interaction with other organelles, thereby regulating lysosomes fuse (*13*). Our findings suggest that PLAC8 may establish nonfusion function in Cd-exposed cells.

We stained Cd-transformed prostate epithelial cells for PLAC8 and found that PLAC8 actively displaces LAMP1 rather than localizing with LC3B. This displacement inhibits the colocalization of LC3B and LAMP1. Moreover, knocking down PLAC8 substantially decreased the expression of LC3B, and LAMP1 restored the interaction between LC3B and LAMP1; it also reestablished the fusion of autophagosomes with lysosomes. These results indicate that although PLAC8 is essential for the autophagy process, it also

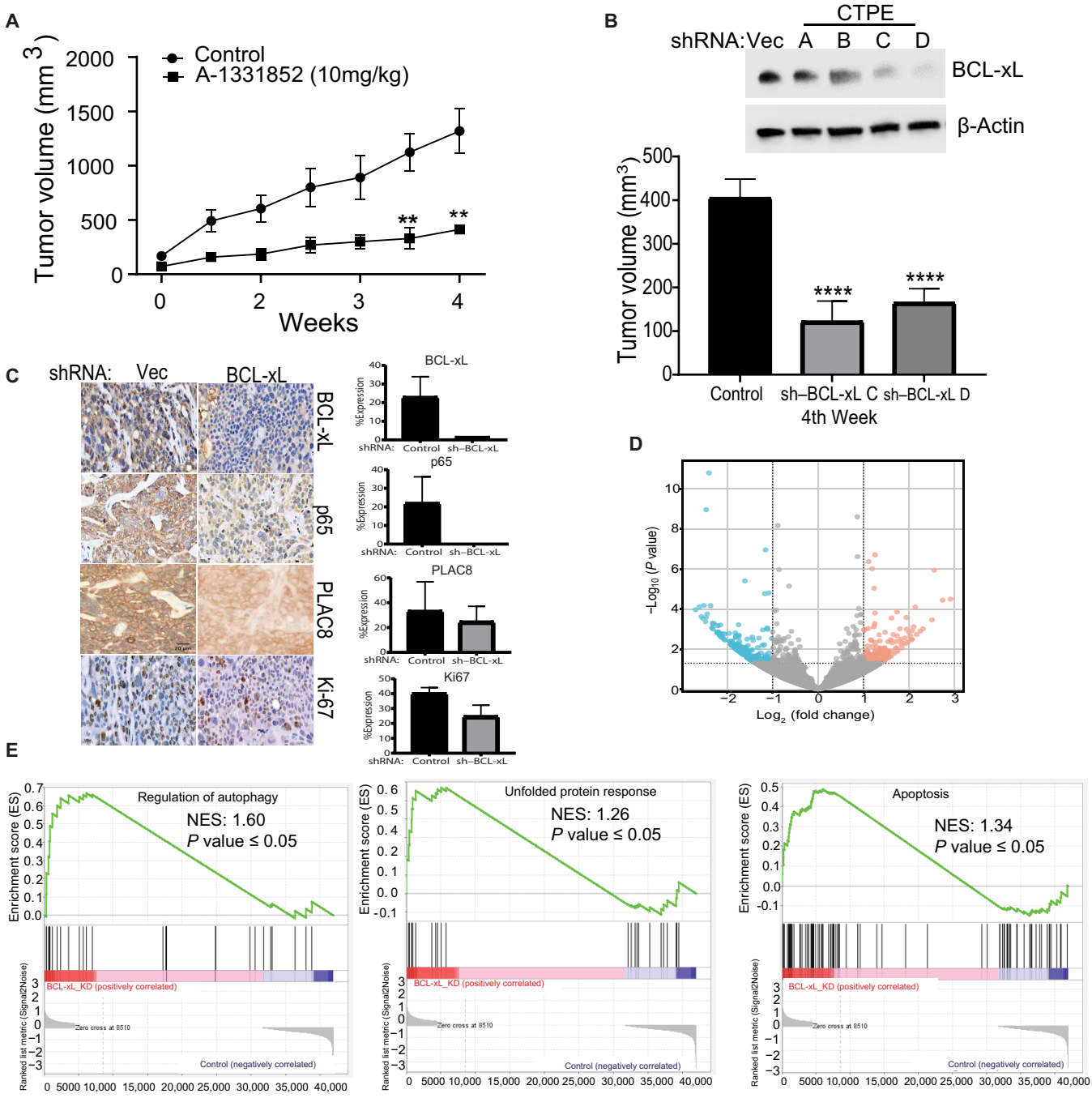

Fig. 6. Inhibition of BCL-xL suppresses PLAC8-mediated tumorigenesis in a xenotransplanted model. (**A**) The intraperitoneal injection of a pharmacological inhibitor of BCL-xL (A-1155643) and (**B**) stably suppressing BCL-xL in CTPE cells significantly inhibits tumor growth. (**C**) IHC analysis of Ki-67, p65, PLAC8, LC3B, and LAMP1 expression in both vector and sh–BCL-xL groups. (**D**) A volcano plot analysis demonstrated the differential expression of genes in the shBCL-xL tumors compared to the vehicle group. (**E**) GSEA revealed alterations in the unfolded protein response, autophagy, and apoptosis pathways in sh–BCL-xL tumors compared to the vector group. All error bars represent means ± SD. $^{**}P < 0.01$ and $^{****}P < 0.0001$.

contributes to defects in the autophagosome-lysosome fusion mechanism, allowing Cd-exposed cells to continue proliferating. PLAC8 promotes cell survival which was confirmed in an in vivo model, where xenografts from Cd-transformed PLAC8 knockdown cells exhibited a lower tumor burden than Cd-transformed cell xenografts.

The extensive pathogenicity of Cd likely arises from its capacity to produce oxidative stress and inflammation (*16*, *17*). Notably, underlying inflammation activates NF-κB during malignant progression, which up-regulates tumor-promoting cytokines [e.g., interleukin-6 (IL-6) and TNF-α] and survival genes like *BCL-xL* (*18*). Conversely, PLAC8 can suppress the production of proinflammatory

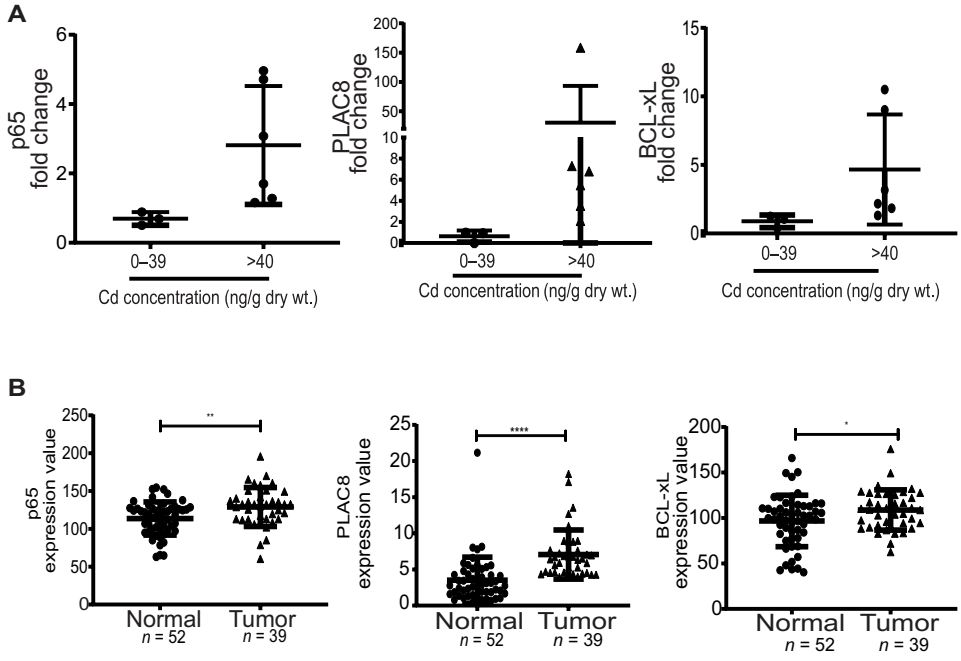

Fig. 7. Validation p65, PLAC8, and BCL-xL expression in prostate cancer specimens. (**A**) On the basis of the Cd levels, reverse transcription qPCR was performed to validate p65, PLAC8, and BCL-xL mRNA expression levels in prostate cancer specimens. wt., weight. (**B**) Expression analysis of p65, PLAC8, and BCL-xL was conducted using TCGA PRAD patients' datasets. Statistical significance levels are $*P < 0.05$, $**P < 0.01$, and $****P < 0.0001$.

cytokines IL-1β and IL-18 by enhancing autophagy (*35*). NF-κB thus establishes a crucial link between inflammation and cancer. NF-κB activation can also stimulate the autophagy pathway (*36*), but the effects of NF-κB on autophagy can vary depending on the cellular context and the duration and intensity of its activity; it can act either as an autophagy inhibitor or an activator (*37*). Thus, tight regulation of the NF-κB pathway and the autophagy process is vital for maintaining cellular homeostasis. We found that NF-κB and BCL-xL expression increased in Cd-exposed RWPE-1 (transforming) cells; that NF-κB accumulates in the nucleus; and that NF-κB and PLAC8 colocalize in the nuclei of transforming cells. We then identified two NF-κB binding sites in the *PLAC8* promoter and mutating these sites diminished PLAC8 function. A ChIP-qPCR assay confirmed direct binding between NF-κB and *PLAC8* in Cd-transformed cells but not in control RWPE-1 cells. We confirmed that PLAC8-mediated expression of crucial autophagy markers relies on NF-κB activation by knocking down NF-κB (*p65*) in Cd-transformed cells and showing that xenografts with *p65* knockdown had substantially reduced autophagy marker expression and tumor burden. Thus, NF-κB is a primary driver of autophagy signaling in Cd-transformed prostate epithelial cells.

When we overexpressed *PLAC8* in RWPE-1 cells, we also saw increased BCL-xL levels. Previous studies have established that induction of BCL-xL expression governs cell survival under oncogenic stress in different cancer cell types (*38*). While it is known that NF-κB regulates BCL-xL (*39*), our findings reveal a reciprocal relationship: BCL-xL also influences NF-κB expression. Acute Cd exposure leads to oxidative stress and DNA damage, frequently resulting in apoptosis. However, Cd-transformed cells are more likely to accumulate genetic alterations that enable them to withstand various stresses. In addition, BCL-xL–mediated survival signaling helps these cells evade apoptosis, potentially leading to survival of malignant cells. Studies have demonstrated that BCL-xL can delay the onset of lead-induced apoptosis (*40*, *41*). Our research has observed a concurrent induction of BCL-xL and PLAC8 in Cd-transformed cells, suggesting that BCL-xL may confer a survival advantage since there was no change in the expression of other prosurvival markers, such as BCL2. In addition, the ectopic expression of PLAC8 in normal prostate cells induced BCL-xL, indicating a molecular interplay between these two proteins. Moreover, the regulation of BCL-xL by PLAC8 was confirmed in Cd-transformed cells and normal prostate epithelial cells ectopically overexpressing PLAC8. While these studies strongly support the interaction between PLAC8 and BCL-xL, we cannot dismiss the potential involvement of additional mechanisms in regulating BCL-xL. For instance, PLAC8 activates CCAAT/enhancer binding protein (C/EBP) transcription factors (*42*), which may also enhance BCL-xL expression (*43*), and we observed an up-regulation of C/EBP in transformed cells and those overexpressing PLAC8. This finding suggests that PLAC8 may directly or indirectly activate BCL-xL through C/EBP, thus warranting further investigation.

Our in vitro and in vivo results were corroborated in patient prostate tumors, in that prostate tumors with high Cd levels exhibited increased expression of NF-κB, *PLAC8*, and *BCL-xL* relative to those tumors with low Cd levels. Although the clinical sample size was relatively small, these findings align with other studies indicating that Cd exposure induces oxidative stress and activate signaling pathways associated with cancer progression (*44*). In summary, then, we offer experimental and preclinical evidence for how autophagy and survival mechanisms are regulated in Cd-transformed prostate epithelial cells and tumors. Our findings indicate that Cd up-regulates

NF-κB, which, in turn, up-regulates PLAC8 and stabilizes PLAC8 in the cytoplasm. PLAC8 substitutes for LAMP1 and inhibits the fusion of autophagosomes with lysosomes. The interactions between NF-κB and PLAC8 alter the expression of downstream, autophagy-related genes (i.e., *BCL-xL*). Knocking down NF-κB in transformed cells replicated the effects seen with *PLAC8* knockdown, eliminating the survival advantage conferred by BCL-xL. NF-κB knockdown triggered programmed cell death pathways (including autophagy and apoptosis), ultimately leading to cell death and tumor regression. Disrupting any of these molecules counteracts these effects in vitro and in vivo. We have therefore uncovered an oncogenic axis linking NF-κB, PLAC8, and BCL-xL, which should encourage further collaboration and discussion to identify new prostate cancer therapies.

MATERIALS AND METHODS

Cell lines and reagents

Human normal prostate epithelial (RWPE-1) cells were purchased from the American Type Culture Collection (VA, USA) and subcultured with the recommended protocol. Cd chloride hydrate (0.1 M) was purchased from Hampton Research (USA), CHX was purchased from Sigma-Aldrich (St. Louis, USA), BD Matrigel was purchased from Corning (NY, USA), A-1331852 (BCL_{xL} inhibitor) was purchased from MedChemExpress (NJ, USA), and LPS was purchased from Sigma-Aldrich (St. Louis, USA).

shRNA/small interfering RNA/pCMV transfections

Cd-transformed RWPE-1 cells with stable *PLAC8* (TL302451, Origene), NF-κB (TL302038, Origene), or *BCL-xL* (TR320077, Origene) knockdown were generated by shRNA and antibiotic selection. *BCL-xL* (6362, Cell Signaling) or a control small interfering RNA was used for transient transfection. For overexpression studies, RWPE-1 cells were transiently transfected with a *PLAC8* (RC212588, Origene), NF-κB (RC220780, Origene), or *BCL-xL* (RC201314, Origene) expression plasmid, using Lipofectamine 2000 (Thermo Fisher Scientific, USA) as transfection reagent according to the manufacturer's instructions. Immunoblotting was performed to confirm the knockdown or overexpression.

Protein extraction and Western blots

RWPE-1 and CTPE cells were seeded in six-well plates, incubated for 24 hours, and then treated with Cd (10 μM) for up to 72 hours. Lysates were prepared using radioimmunoprecipitation assay buffer (Sigma-Aldrich, supplemented with protease and phosphatase inhibitor cocktail (Thermo Fisher Scientific, USA). Protein concentrations were quantified using a Pierce BCL Protein Assay Kit (Thermo Fisher Scientific, USA). Western blots were performed using antibodies against PLAC8 (ab122652, Abcam), NF-κB (8242, Cell signaling), LC3B (ab51520, abcam), LAMP1 (9091, Cell Signaling), BCL-xL (2764, Cell Signaling), BCL-2 (2872, Cell Signaling), and β-actin (5125, Cell Signaling). Protein-antibody complexes were visualized using a ChemiDOC MP (Bio-Rad, USA).

Cyclohexamide treatment

After transfecting cells with shNF-κB and confirming knockdown by Western blot, cells were treated with 50 μM CHX for 0, 3, 6, and 12 hours. After treatment, cell lysates were prepared for immunoblotting, as described before (*45*).

Nuclear and cytoplasmic extractions

Nuclear and cytoplasmic fractions of successive stages of transforming cells were extracted with a NE-PER Nuclear and Cytoplasmic Extraction Reagent according to the manufacturer's instructions (Thermo Fisher Scientific, USA).

Immunoprecipitation

Immunoprecipitation experiments were performed with Pierce Protein A/G Plus agarose (Thermo Fisher Scientific, USA), which was incubated with 50 μg of cell lysate and anti-NF-κB antibody (8242, Cell Signaling) overnight at 40°C. Proteins were resolved by SDS–polyacrylamide gel electrophoresis (Bio-Rad, USA) and detected by Western blot.

NF-κB activity

The DNA binding activity of NF-κB was analyzed by the NF-κB p65 Transcription Factor Assay Kit (ab133112, Abcam), and NF-κB nuclear translocation was determined by Western blot. All experiments were performed in three technical replicates.

Immunofluorescence analysis

RWPE-1 and CTPE cells were seeded on Falcon eight-well culture slides (Corning, USA) and grown to ~60% confluence, as previously described (*15*). After treating cells with vehicle or Cd for 24 hours, cells were washed and then incubated with PLAC8 (ab122652, Abcam), NF-κB (8242, Cell Signaling), LC3b (ab243506 and ab51520, Abcam), and/or LAMP1 (ab25630, Abcam) antibodies, followed by secondary antibodies conjugated to Alexa Fluor 488 (Green), Alexa Fluor 594, and Alexa Fluor 647 (Thermo Fisher Scientific, USA), respectively. The location of the antigen-antibody complexes was visualized using a Keyence BZ-X8000 microscope (IL, USA). To colocate proteins within individual cells, we used conjugated antibodies for LC3B (ab225383 and ab225382), LAMP1 (ab302684), and NF-κB (ab190589 and ab214846) from Abcam, USA and a PLAC8 antibody (CSB-CSB-PA873705LC01HU) from CUSABIO, USA. Confocal images were captured with a Luminosa microscope (PicoQuant; Berlin, Germany), and Pearson coefficients were calculated using ImageJ and the JACoP plugin (*46*).

Transmission electron microscopy

Cells were fixed in 2.5% glutaraldehyde and 0.1 M sodium cacodylate buffer (pH 7.4) for 1 hour at room temperature and stored at 4°C. They were subsequently washed in 0.15 M sodium phosphate buffer, treated with reduced osmium tetroxide for 1 hour, washed with deionized water, and dehydrated in graded ethanol and propylene oxide. Samples were infiltrated with propylene oxide 812 epoxy resin, cured at 60°C, and sectioned at 80 nm. Sections on copper grids were stained with 4% uranyl acetate and Reynold's lead citrate as described before (*47*). Samples were viewed using a JEOL JEM-1230 transmission electron microscope operating at 80 kV (JEOL USA Inc., Peabody, MA), and images were obtained using a Gatan Orius SC1000 charge-coupled device digital camera and Gatan Microscopy Suite 3.0 software (Gatan Inc., Pleasanton, CA). Resulting images were analyzed in ImageJ as described elsewhere (*48*), with the autophagic compartments identified as indicated in (*49*, *50*).

Dual luciferase assay

Interactions between p65 and the *PLAC8* promoter were detected using a dual-luciferase reporter assay. The Gaussia luciferase vector

(Gluc) plasmid containing wild-type *PLAC8*, mutant (Δ) *PLAC8*, or wild-type *BCL-xL* promoter sequences was constructed by GeneCopoeia (USA). Plasmids were then transfected into RWPE-1 or CTPE cells. LPS (1 μg/ml) was used to induce NF-κB expression, as described before (*51*). The relative luciferase activity was quantified using the Secrete-pair Dual Luminescence Assay Kit (GeneCopoeia, USA).

Clinical samples

Nine prostate cancer tissue samples were obtained from the University of Louisville and Robley Rex Department of Veterans Affairs Medical Center with the approval of the Committee for the Protection of Human Subjects in Research. Every participant in the study was interviewed, and prostate tissues were taken with their consent.

Real-time quantitative PCR

Total RNA was isolated from cell lines and clinical specimens using the Qiagen's RNeasy Kit (Hilden, Germany) and then treated with deoxyribonuclease I (Thermo Fisher Scientific, USA). RNA was reverse transcribed using the iScript Reverse Transcription Supermix (Bio-Rad, USA), and qPCR was performed using the primers in table S1 and the SsoAdvanced Universal SYBR Green Supermix (Bio-Rad, USA). The expression level of each gene was calculated after normalizing with β-actin gene expression. ChIP-qPCR was performed with the NF-κB antibody (8242, Cell Signaling) and the high-sensitivity ChiP Kit (Abcam, UK) according to the manufacturer's protocol, using ChIP-qPCR primers listed in table S1. All experiments were performed in three technical replicates.

Cell viability, apoptosis, and soft agar colony formation assays

Cells were first transfected with *p65*, *BCL-xL*, or scrambled shRNAs. Alamar blue (Thermo Fisher Scientific, USA) and EdU cell proliferation (Sigma-Aldrich, USA) assays were then performed per the manufacturer's instructions. We used an annexin V–FITC Apoptosis Kit-I (BD Pharmingen, San Diego, CA) for apoptosis assays, as described previously (*15*). Colony formation assays used the CytoSelect 96-Well In Vitro Tumor Sensitivity Assay Kit (Cell Biolabs Inc., USA), as previously described (*15*).

Xenograft studies and in vivo treatments

PLAC8, NF-κB, and BCL-xL shRNA-transfected cells (~1.5×10^6 cells in 1:1 Matrigel) were subcutaneously injected into separate flanks of 6- to 8-week-old BALB/c athymic nude mice (the Jackson Laboratory, strain no. 002019). The study was approved by the University Laboratory Animal Care Committee of University of Louisville and Texas A&M University [animal use protocol (AUP): Institutional Animal Care and use committee (IACUC)]. Animals were monitored daily, and tumor size was measured twice per week as previously described (*15*). After 4 weeks, mice were euthanized, and the tumor xenografts were collected for subsequent experiments. For the pharmacological experiment, ~1.5×10^6 Cd-transformed RWPE-1 cells (in 1:1 Matrigel) were subcutaneously injected into nude mice, and tumor growth was measured every 2 days. When the tumor volumes reached >100 mm^3, mice were randomized into two groups. One group was injected subcutaneously with vehicle [10% dimethyl sulfoxide (DMSO)/90% saline], and the other group was injected with A-1331852 (10 mg/kg) in 10% DMSO/90% saline. Animals were treated with vehicle or A-1331852 twice per week for 4 weeks. When tumors in the control group reached 1000 to 1200 mm^3, all animals were euthanized, and the tumors were harvested for subsequent experiments.

Immunohistochemistry

Xenograft tumors were fixed in 10% formalin and processed for immunohistochemistry (IHC) as described previously (36764624), using PLAC8 (ab122652, Abcam), NF-κB (8242, Cell Signaling), BCL-xL (2764, Cell Signaling), LC3B (ab51520, Abcam), LAMP1 (9091, Cell signaling), and Ki67 (ab15580, Abcam) antibodies. Images (40×) were captured with an Olympus BX43 microscope (Olympus America, Center Valley, PA), and protein expression was quantified with the ImageJ software and the DeConvolution 2 plugin as described elsewhere (*52*).

RNA sequencing

Total RNA was isolated from xenograft tumors ($n = 2$) using a SV Total RNA Isolation System (Promega, USA). Isolated RNA was enriched for mRNA using a QuantSeq 3′ mRNA-seq library prep kit (Lexogen, Austria), followed by cDNA conversion and library preparation. The sequencing was performed using an Illumina NextSeq500 platform (CA, USA). Library preparation and sequencing were performed by Lexogen NGS services (Vienna, Austria).

TCGA data and bioinformatic analysis

Reads were aligned to a reference genome using STAR (*53*), with quality metrics obtained from the RSeQC quality control package (*54*). We use DeSeq2 (*55*) for differential gene expression analysis. Up-regulated genes were defined by $\log_2(FC) > 1$ with $P < 0.05$, and down-regulated genes were defined by $\log_2(FC) \leq 1$ and $P < 0.05$. To investigate the expression levels of *PLAC8*, NF-κB, and *BCL-xL* in patients with prostate cancer, we retrieved data from TCGA Program datasets using cBioPortal (*56*) and extracted gene expression values from OncoDB (*57*).

Functional enrichment analysis

To functionally annotate the list of genes and calculate the normalized enrichment score, GSEA was performed (*58*). The volcano plot was generated using SRplot (*59*).

Cd measurement method

Twenty milligrams of dry prostate tissue was digested with nitric acid for 30 min at 90°C. After digestion, the tissue samples were left to dry at 50°C overnight. Once cooled to room temperature, the samples were diluted with Milli-Q water to ascertain their metal concentration, as previously demonstrated by Neslund-Dudas *et al.* (*17*) and Tyagi *et al.* (*23*). The analysis was carried out using a PerkinElmer NexION 200C (Waltham, MA). Concentrations were expressed as nanograms per gram of dry tissue weight.

Statistical analysis

Statistical analyses were performed using GraphPad Prism 6.0a software (GraphPad Software Inc., La Jolla, CA). Results are expressed as means ± SEM. Datasets were compared using a two-tailed unpaired Student's *t* test. Statistical significance was set at $P < 0.05$. All experiments were performed in two biological replicates.

Supplementary Materials

This PDF file includes:

Figs. S1 to S21
Tables S1 to S5

REFERENCES AND NOTES

1. D. J. Klionsky, F. C. Abdalla, H. Abeliovich, R. T. Abraham, A. Acevedo-Arozena, K. Adeli, L. Agholme, M. Agnello, P. Agostinis, J. A. Aguirre-Ghiso, H. J. un Ahn, O. Ait-Mohamed, S. Ait-Si-Ali, T. Akematsu, S. Akira, H. M. Al-Younes, M. A. Al-Zeer, M. L. Albert, R. L. Albin, J. Alegre-Abarrategui, M. F. rancesca Aleo, M. Alirezaei, A. Almasan, M. Almonte-Becerril, A. Amano, R. Amaravadi, S. Amarnath, A. O. Amer, N. Andrieu-Abadie, V. Anantharam, D. K. Ann, S. Anoopkumar-Dukie, H. Aoki, N. Apostolova, G. Arancia, J. P. Aris, K. Asanuma, N. Y. O. Asare, H. Ashida, V. Askanas, D. S. Askew, P. Auberger, M. Baba, S. K. Backues, E. H. Baehrecke, B. A. Bahr, X. Y. Bai, Y. Bailly, R. Baiocchi, G. Baldini, W. Balduini, A. Ballabio, B. A. Bamber, E. T. W. Bampton, G. Bánhegyi, C. R. Bartholomew, D. C. Bassham, R. C. Bast, H. Batoko, B. H. Bay, I. Beau, D. M. Béchet, T. J. Begley, C. Behl, C. Behrends, S. Bekri, B. Bellaire, L. J. Bendall, L. Benetti, L. Berliocchi, H. Bernardi, F. Bernassola, S. Besteiro, I. Bhatia-Kissova, X. Bi, M. Biard-Piechaczyk, J. S. Blum, L. H. Boise, P. Bonaldo, D. L. Boone, B. C. Bornhauser, K. R. Bortoluci, I. Bossis, F. Bost, J. P. Bourquin, P. Boya, M. Boyer-Guittaut, P. V. Bozhkov, N. R. Brady, C. Brancolini, A. Brech, J. E. Brenman, A. Brennand, E. H. Bresnick, P. Brest, D. Bridges, M. L. Bristol, P. S. Brookes, E. J. Brown, J. H. Brumell, N. Brunetti-Pierri, U. T. Brunk, D. E. Bulman, S. J. Bultman, G. Bultynck, L. F. Burbulla, W. Bursch, J. P. Butchar, W. Buzgariu, S. P. Bydlowski, K. Cadwell, M. Cahová, D. Cai, J. Cai, Q. Cai, B. Calabretta, J. Calvo-Garrido, N. Camougrand, M. Campanella, J. Campos-Salinas, E. Candi, L. Cao, A. B. Caplan, S. R. Carding, S. M. Cardoso, J. S. Carew, C. R. Carlin, V. Carmignac, L. A. M. Carneiro, S. Carra, R. A. Caruso, G. Casari, C. Casas, R. Castino, E. Cebollero, F. Cecconi, J. Celli, H. Chaachouay, H. J. Chae, C. Y. Chai, D. C. Chan, E. Y. Chan, R. C.-C. Chang, C. M. Che, C. C. Chen, G. C. Chen, G. Q. Chen, M. Chen, Q. Chen, S. S. L. Chen, W. L. Chen, X. Chen, X. Chen, X. Chen, Y. G. Chen, Y. Chen, Y. Chen, Y. J. Chen, Z. Chen, A. Cheng, C. H. K. Cheng, Y. Cheng, H. Cheong, J. H. Cheong, S. Cherry, R. Chess-Williams, Z. H. Cheung, E. Chevet, H. L. Chiang, R. Chiarelli, T. Chiba, L. S. Chin, S. H. Chiou, F. V. Chisari, C. H. Cho, D. H. Cho, A. M. K. Choi, D. S. Choi, K. S. ook Choi, M. E. Choi, S. Chouaib, D. Choubey, V. Choubey, C. T. Chu, T. H. Chuang, S. H. Chueh, T. Chun, Y. J. Chwae, M. L. Chye, R. Ciarcia, M. R. Ciriolo, M. J. Clague, R. S. B. Clark, P. G. H. Clarke, R. Clarke, P. Codogno, H. A. Coller, M. I. Colombo, S. Comincini, M. Condello, F. Condorelli, M. R. Cookson, G. H. Coombs, I. Coppens, R. Corbalan, P. Cossart, P. Costelli, S. Costes, A. Coto-Montes, E. Couve, F. P. Coxon, J. M. Cregg, J. L. Crespo, M. J. Cronjé, A. M. Cuervo, J. J. Cullen, M. J. Czaja, M. D'Amelio, A. Darfeuille-Michaud, L. M. Davids, F. E. Davies, M. De Felici, J. F. de Groot, C. A. M. de Haan, L. De Martino, A. De Milito, V. De Tata, J. Debnath, A. Degterev, B. Dehay, L. M. D. Delbridge, F. Demarchi, Y. Z. Deng, J. Dengjel, P. Dent, D. Denton, V. Deretic, S. D. Desai, R. J. Devenish, M. Di Gioacchino, G. Di Paolo, C. Di Pietro, G. Díaz-Araya, I. Díaz-Laviada, M. T. Diaz-Meco, J. Diaz-Nido, I. Dikic, S. P. Dinesh-Kumar, W. X. Ding, C. W. Distelhorst, A. Diwan, M. Djavaheri-Mergny, S. Dokudovskaya, Z. Dong, F. C. Dorsey, V. Dosenko, J. J. Dowling, S. Doxsey, M. Dreux, M. E. Drew, Q. Duan, M. A. Duchosal, K. Duff, I. Dugail, M. Durbeej, M. Duszenko, C. L. Edelstein, A. L. Edinger, G. Egea, L. Eichinger, N. T. Eissa, S. Ekmekcioglu, W. S. El-Deiry, Z. Elazar, M. Elgendy, L. M. Ellerby, K. E. Eng, A. M. Engelbrecht, S. Engelender, J. Erenpreisa, R. Escalante, A. Esclatine, E. L. Eskelinen, L. Espert, V. Espina, H. Fan, J. Fan, Q. W. Fan, Z. Fan, S. Fang, Y. Fang, M. Fanto, A. Fanzani, T. Farkas, J. C. Farré, M. Faure, M. Fechheimer, C. G. Feng, J. Feng, Q. Feng, Y. Feng, L. Fésüs, R. Feuer, M. E. Figueiredo-Pereira, G. M. Fimia, D. C. Fingar, S. Finkbeiner, T. Finkel, K. D. Finley, F. Fiorito, E. A. Fisher, P. B. Fisher, M. Flajolet, M. L. Florez-McClure, S. Florio, E. A. Fon, F. Fornai, F. Fortunato, R. Fotedar, D. H. Fowler, H. S. Fox, R. Franco, L. B. Frankel, M. Fransen, J. M. Fuentes, J. Fueyo, J. Fujii, K. Fujisaki, E. Fujita, M. Fukuda, R. H. Furukawa, M. Gaestel, P. Gailly, M. Gajewska, B. Galliot, V. Galy, S. Ganesh, B. Ganetzky, I. G. Ganley, F. B. Gao, G. F. Gao, J. Gao, L. Garcia, G. Garcia-Manero, M. Garcia-Marcos, M. Garmyn, A. L. Gartel, E. Gatti, M. Gautel, T. R. Gawriluk, M. E. Gegg, J. Geng, M. Germain, J. E. Gestwicki, D. A. Gewirtz, S. Ghavami, P. Ghosh, A. M. Giammarioli, A. N. Giatromanolaki, S. B. Gibson, R. W. Gilkerson, M. L. Ginger, H. N. Ginsberg, J. Golab, M. S. Goligorsky, P. Golstein, C. Gomez-Manzano, E. Goncu, C. Gongora, C. D. Gonzalez, R. Gonzalez, C. González-Estévez, R. A. González-Polo, E. Gonzalez-Rey, N. V. Gorbunov, S. Gorski, S. Goruppi, R. A. Gottlieb, D. Gozuacik, G. E. Granato, G. D. Grant, K. N. Green, A. Gregorc, F. Gros, C. Grose, T. W. Grunt, P. Gual, J. L. Guan, K. L. Guan, S. M. Guichard, A. S. Gukovskaya, I. Gukovsky, J. Gunst, A. B. Gustafsson, A. J. Halayko, A. N. Hale, S. K. Halonen, M. Hamasaki, F. Han, T. Han, M. K. Hancock, M. Hansen, H. Harada, M. Harada, S. E. Hardt, J. W. Harper, A. L. Harris, J. Harris, S. D. Harris, M. Hashimoto, J. A. Haspel, S.-i. Hayashi, L. A. Hazelhurst, C. He, Y. W. He, M. J. Hébert, K. A. Heidenreich, M. H. Helfrich, G. V. Helgason, E. P. Henske, B. Herman, P. K. Herman, C. Hetz, S. Hilfiker, J. A. Hill, L. J. Hocking, P. Hofman, T. G. Hofmann, J. Höhfeld, T. L. Holyoake, M. H. Hong, D. A. Hood, G. S. Hotamisligil, E. J. Houwerzijl, M. Høyer-Hansen, B. Hu, C. A. A. Hu, H. M. Hu, Y. Hua, C. Huang, J. Huang, S. Huang, W. P. Huang, T. B. Huber, W. K. Huh, T. H. Hung, T. R. Hupp, G. M. in Hur, J. B. Hurley, S. N. A. Hussain, P. J. Hussey, J. J. in Hwang, S. Hwang, A. Ichihara, S. Ilkhanizadeh, K. Inoki, T. Into, V. Iovane, J. L. Iovanna, N. Y. Ip, Y. Isaka, H. Ishida, C. Isidoro, K.-i. Isobe, A. Iwasaki, M. Izquierdo, Y. Izumi, P. M. Jaakkola, M. Jäättelä, G. R. Jackson, W. T. Jackson, B. Janji, M. Jendrach, J. H. Jeon, E. B. Jeung, H. Jiang, H. Jiang, J. X. Jiang, M. Jiang, Q. Jiang, X. Jiang, A. Jiménez, M. Jin, S. Jin, C. O. Joe, T. Johansen, D. E. Johnson, G. V. W. Johnson, N. L. Jones, B. Joseph, S. K. Joseph, A. M. Joubert, G. Juhász, L. Juillerat-Jeanneret, C. H. Jung, Y. K. Jung, K. Kaarniranta, A. Kaasik, T. Kabuta, M. Kadowaki, K. Kagedal, Y. Kamada, V. O. Kaminskyy, H. H. Kampinga, H. Kanamori, C. Kang, K. B. Kang, K. I. Kang, R. Kang, Y. A. Kang, T. Kanki, T. D. Kanneganti, H. Kanno, A. G. Kanthasamy, A. Kanthasamy, V. Karantza, G. P. Kaushal, S. Kaushik, Y. Kawazoe, P. Y. Ke, J. H. Kehrl, A. Kelekar, C. Kerkhoff, D. H. Kessel, H. Khalil, J. A. K. W. Kiel, A. A. Kiger, A. Kihara, D. R. Kim, D. H. Kim, D. H. Kim, E. K. Kim, H. R. Kim, J. S. Kim, J. H. Kim, J. C. Kim, J. K. Kim, P. K. Kim, S. W. Kim, Y. S. Kim, Y. Kim, A. Kimchi, A. C. Kimmelman, J. S. King, T. J. Kinsella, V. Kirkin, L. A. Kirshenbaum, K. Kitamoto, K. Kitazato, L. Klein, W. T. Klimecki, J. Klucken, E. Knecht, B. C. B. Ko, J. C. Koch, H. Koga, J. Y. Koh, Y. H. Koh, M. Koike, M. Komatsu, E. Kominami, H. J. Kong, W. J. Kong, V. I. Korolchuk, Y. Kotake, M. I. Koukourakis, J. B. K. Flores, A. L. Kovács, C. Kraft, D. Krainc, H. Krämer, C. Kretz-Remy, A. M. Krichevsky, G. Kroemer, R. Krüger, O. Krut, N. T. Ktistakis, C. Y. Kuan, R. Kucharczyk, A. Kumar, R. Kumar, S. Kumar, M. Kundu, H. J. Kung, T. Kurz, H. J. Kwon, A. R. La Spada, F. Lafont, T. Lamark, J. Landry, J. D. Lane, P. Lapaquette, J. F. Laporte, L. László, S. Lavandero, J. N. Lavoie, R. Layfield, P. A. Lazo, W. Le, L. Le Cam, D. J. Ledbetter, A. J. X. Lee, B. W. Lee, G. M. in Lee, J. Lee, J. H. Lee, M. Lee, M. S. Lee, S. H. Lee, C. Leeuwenburgh, P. Legembre, R. Legouis, M. Lehmann, H. Y. Lei, Q. Y. Lei, D. A. Leib, J. Leiro, J. J. Lemasters, A. Lemoine, M. S. Lesniak, D. Lev, V. V. Levenson, B. Levine, E. Levy, F. Li, J. L. Li, L. Li, S. Li, W. Li, X. J. Li, Y. Li, Y. P. Li, C. Liang, Q. Liang, Y. F. Liao, P. P. Liberski, A. Lieberman, H. J. Lim, K. L. Lim, K. Lim, C. F. Lin, F. C. Lin, J. Lin, J. D. Lin, K. Lin, W. W. Lin, W. C. Lin, Y. L. Lin, R. Linden, P. Lingor, J. Lippincott-Schwartz, M. P. Lisanti, P. B. Liton, B. Liu, C. F. Liu, K. Liu, L. Liu, Q. A. Liu, W. Liu, Y. C. Liu, Y. Liu, R. A. Lockshin, C. N. Lok, S. Lonial, B. Loos, G. Lopez-Berestein, C. López-Otín, L. Lossi, M. T. Lotze, P. Lőw, B. Lu, B. Lu, B. Lu, Z. Lu, F. Luciano, N. W. Lukacs, A. H. Lund, M. A. Lynch-Day, Y. Ma, F. Macian, J. P. MacKeigan, K. F. Macleod, F. Madeo, L. Maiuri, M. C. Maiuri, D. Malagoli, M. C. V. Malicdan, W. Malorni, N. Man, E. M. Mandelkow, S. Manon, I. Manov, K. Mao, X. Mao, Z. Mao, P. Marambaud, D. Marazziti, Y. L. Marcel, K. Marchbank, P. Marchetti, S. J. Marciniak, M. Marcondes, M. Mardi, G. Marfe, G. Mariño, M. Markaki, M. R. Marten, S. J. Martin, C. Martinand-Mari, W. Martinet, M. Martinez-Vicente, M. Masini, P. Matarrese, S. Matsuo, R. Matteoni, A. Mayer, N. M. Mazure, D. J. McConkey, M. J. McConnell, C. McDermott, C. McDonald, G. M. McInerney, S. L. McKenna, B. A. McLaughlin, P. J. McLean, C. R. McMaster, G. A. McQuibban, A. J. Meijer, M. H. Meisler, A. Meléndez, T. J. Melia, G. Melino, M. A. Mena, J. A. Menendez, R. F. S. Menna-Barreto, M. B. Menon, F. M. Menzies, C. A. Mercer, A. Merighi, D. E. Merry, S. Meschini, C. G. Meyer, T. F. Meyer, C. Y. Miao, J. Y. Miao, P. A. M. Michels, C. Michiels, D. Mijaljica, A. Milojkovic, S. Minucci, C. Miracco, C. K. Miranti, I. Mitroulis, K. Miyazawa, N. Mizushima, B. Mograbi, S. Mohseni, X. Molero, B. Mollereau, F. Mollinedo, T. Momoi, I. Monastyrska, M. M. Monick, M. J. Monteiro, M. N. Moore, R. Mora, K. Moreau, P. I. Moreira, Y. Moriyasu, J. Moscat, S. Mostowy, J. C. Mottram, T. Motyl, C. E. H. Moussa, S. Müller, S. Muller, K. Münger, C. Münz, L. O. Murphy, M. E. Murphy, A. Musarò, I. Mysorekar, E. Nagata, K. Nagata, A. Nahimana, U. Nair, T. Nakagawa, K. Nakahira, H. Nakano, H. Nakatogawa, M. Nanjundan, N. I. Naqvi, D. P. Narendra, M. Narita, M. Navarro, S. T. Nawrocki, T. Y. Nazarko, A. Nemchenko, M. G. Netea, T. P. Neufeld, P. A. Ney, I. P. Nezis, H. P. Nguyen, D. Nie, I. Nishino, C. Nislow, R. A. Nixon, T. Noda, A. A. Noegel, A. Nogalska, S. Noguchi, L. Notterpek, I. Novak, T. Nozaki, N. Nukina, T. Nürnberger, B. Nyfeler, K. Obara, T. D. Oberley, S. Oddo, M. Ogawa, T. Ohashi, K. Okamoto, N. L. Oleinick, F. J. Oliver, L. J. Olsen, S. Olsson, O. Opota, T. F. Osborne, G. K. Ostrander, K. Otsu, J. J. Ou, M. Ouimet, M. Overholtzer, B. Ozpolat, P. Paganetti, U. Pagnini, N. Pallet, G. E. Palmer, C. Palumbo, T. Pan, T. Panaretakis, U. B. Pandey, Z. Papackova, I. Papassideri, I. Paris, J. Park, O. K. Park, J. B. Parys, K. R. Parzych, S. Patschan, C. Patterson, S. Pattingre, J. M. Pawelek, J. Peng, D. H. Perlmutter, I. Perrotta, G. Perry, S. Pervaiz, M. Peter, G. J. Peters, M. Petersen, G. Petrovski, J. M. Phang, M. Piacentini, P. Pierre, V. Pierrefite-Carle, G. Pierron, R. Pinkas-Kramarski, A. Piras, N. Piri, L. C. Platanias, S. Pöggeler, M. Poirot, A. Poletti, C. Poüs, M. Pozuelo-Rubio, M. Prætorius-Ibba, A. Prasad, M. Prescott, M. Priault, N. Produit-Zengaffinen, A. Progulske-Fox, T. Proikas-Cezanne, S. Przedborski, K. Przyklenk, R. Puertollano, J. Puyal, S. B. Qian, L. Qin, Z. H. Qin, S. E. Quaggin, N. Raben, H. Rabinowich, S. W. Rabkin, I. Rahman, A. Rami, G. Ramm, G. Randall, F. Randow, V. A. Rao, J. C. Rathmell, B. Ravikumar, S. K. Ray, B. H. Reed, J. C. Reed, F. Reggiori, A. Régnier-Vigouroux, A. S. Reichert, J. J. Reiners, R. J. Reiter, J. Ren, J. L. Revuelta, C. J. Rhodes, K. Ritis, E. Rizzo, J. Robbins, M. Roberge, H. Roca, M. C. Roccheri, S. Rocchi, H. P. Rodemann, S. R. de Córdoba, B. Rohrer, I. B. Roninson, K. Rosen, M. M. Rost-Roszkowska, M. Rouis, K. M. A. Rouschop, F. Rovetta, B. P. Rubin, D. C. Rubinsztein, K. Ruckdeschel, E. B. Rucker, A. Rudich, E. Rudolf, N. Ruiz-Opazo, R. Russo, T. E. Rusten, K. M. Ryan, S. W. Ryter, D. M. Sabatini, J. Sadoshima, T. Saha, T. Saitoh, H. Sakagami, Y. Sakai, G. H. Salekdeh, P. Salomoni, P. M. Salvaterra, G. Salvesen, R. Salvioli, A. M. J. Sanchez, J. A. Sánchez-Alcázar, R. Sánchez-Prieto, M. Sandri, U. Sankar, P. Sansanwal, L. Santambrogio, S. Saran, S. Sarkar,

M. Sarwal, C. Sasakawa, A. Sasnauskiene, M. Sass, K. Sato, M. Sato, A. H. V. Schapira, M. Scharl, H. M. Schätzl, W. Scheper, S. Schiaffino, C. Schneider, M. E. Schneider, R. Schneider-Stock, P. V. Schoenlein, D. F. Schorderet, C. Schüller, G. K. Schwartz, L. Scorrano, L. Sealy, P. O. Seglen, J. Segura-Aguilar, I. Seiliez, O. Seleverstov, C. Sell, J. B. Seo, D. Separovic, V. Setaluri, T. Setoguchi, C. Settembre, J. J. Shacka, M. Shanmugam, I. M. Shapiro, E. Shaulian, R. J. Shaw, J. H. Shelhamer, H. M. Shen, W. C. Shen, Z. H. Sheng, Y. Shi, K. Shibuya, Y. Shidoji, J. J. Shieh, C. M. Shih, Y. Shimada, S. Shimizu, T. Shintani, O. S. Shirihai, G. C. Shore, A. A. Sibirny, S. B. Sidhu, B. Sikorska, E. C. M. Silva-Zacarin, A. Simmons, A. K. Simon, H. U. Simon, C. Simone, A. Simonsen, D. A. Sinclair, R. Singh, D. Sinha, F. A. Sinicrope, A. Sirko, P. M. Siu, E. Sivridis, V. Skop, V. P. Skulachev, R. S. Slack, S. S. Smaili, D. R. Smith, M. S. Soengas, T. Soldati, X. Song, A. K. Sood, T. W. Soong, F. Sotgia, S. A. Spector, C. D. Spies, W. Springer, S. M. Srinivasula, L. Stefanis, J. S. Steffan, R. Stendel, H. Stenmark, A. Stephanou, S. T. Stern, C. Sternberg, B. Stork, P. Strålfors, C. S. Subauste, X. Sui, D. Sulzer, J. Sun, S. Y. Sun, Z. J. Sun, J. J. Y. Sung, K. Suzuki, T. Suzuki, M. S. Swanson, C. Swanton, S. T. Sweeney, L. K. Sy, G. Szabadkai, I. Tabas, H. Taegtmeyer, M. Tafani, K. Takács-Vellai, Y. Takano, K. Takegawa, G. Takemura, F. Takeshita, N. J. Talbot, K. S. W. Tan, K. Tanaka, K. Tanaka, D. Tang, D. Tang, I. Tanida, B. A. Tannous, N. Tavernarakis, G. S. Taylor, G. A. Taylor, J. P. Taylor, L. S. Terada, A. Terman, G. Tettamanti, K. Thevissen, C. B. Thompson, A. Thorburn, M. Thumm, F. F. Tian, Y. Tian, G. Tocchini-Valentini, A. M. Tolkovsky, Y. Tomino, L. Tönges, S. A. Tooze, C. Tournier, J. Tower, R. Towns, V. Trajkovic, L. H. Travassos, T. F. Tsai, M. P. Tschan, T. Tsubata, A. Tsung, B. Turk, L. S. Turner, S. C. Tyagi, Y. Uchiyama, T. Ueno, M. Umekawa, R. Umemiya-Shirafuji, V. K. Unni, M. I. Vaccaro, E. M. Valente, G. Van den Berghe, I. J. van der Klei, W. van Doorn, L. F. van Dyk, M. van Egmond, L. A. van Grunsven, P. Vandenabeele, W. P. Vandenberghe, I. Vanhorebeek, E. C. Vaquero, G. Velasco, T. Vellai, J. M. Vicencio, R. D. Vierstra, M. Vila, C. Vindis, G. Viola, M. T. Viscomi, O. V. Voitsekhovskaja, C. von Haefen, M. Votruba, K. Wada, R. Wade-Martins, C. L. Walker, C. M. Walsh, J. Walter, X. B. Wan, A. Wang, C. Wang, D. Wang, F. Wang, F. Wang, G. Wang, H. Wang, H. G. Wang, H. D. Wang, J. Wang, K. Wang, M. Wang, R. C. Wang, X. Wang, X. Wang, Y. J. Wang, Y. Wang, Z. Wang, Z. C. Wang, Z. Wang, D. G. Wansink, D. M. Ward, H. Watada, S. L. Waters, P. Webster, L. Wei, C. C. Weihl, W. A. Weiss, S. M. Welford, L. P. Wen, C. A. Whitehouse, J. L. Whitton, A. J. Whitworth, T. Wileman, J. W. Wiley, S. Wilkinson, D. Willbold, R. L. Williams, P. R. Williamson, B. G. Wouters, C. Wu, D. C. Wu, W. K. K. Wu, A. Wyttenbach, R. J. Xavier, Z. Xi, P. Xia, G. Xiao, Z. Xie, Z. Xie, D.-z. Xu, J. Xu, L. Xu, X. Xu, A. Yamamoto, A. Yamamoto, S. Yamashina, M. Yamashita, X. Yan, M. Yanagida, D. S. Yang, E. Yang, J. M. Yang, S. Y. Yang, W. Yang, W. Y. Yang, Z. Yang, M. C. Yao, T. P. Yao, B. Yeganeh, W. L. Yen, J.-j. Yin, X. M. Yin, O. J. Yoo, G. Yoon, S. Y. Yoon, T. Yorimitsu, Y. Yoshikawa, T. Yoshimori, K. Yoshimoto, H. J. You, R. J. Youle, A. Younes, L. Yu, L. Yu, S. W. Yu, W. H. Yu, Z. M. Yuan, Z. Yue, C. H. Yun, M. Yuzaki, O. Zabirnyk, E. Silva-Zacarin, D. Zacks, E. Zacksenhaus, N. Zaffaroni, Z. Zakeri, H. J. Zeh, S. O. Zeitlin, H. Zhang, H. L. Zhang, J. Zhang, J. P. Zhang, L. Zhang, L. Zhang, M. Y. Zhang, X. D. Zhang, M. Zhao, Y. F. Zhao, Y. Zhao, Z. J. Zhao, X. Zheng, B. Zhivotovsky, Q. Zhong, C. Z. Zhou, C. Zhu, W. G. Zhu, X. F. Zhu, X. Zhu, Y. Zhu, T. Zoladek, W. X. Zong, A. Zorzano, J. Zschocke, B. Zuckerbraun, Guidelines for the use and interpretation of assays for monitoring autophagy. *Autophagy* **8**, 445–544 (2012).

2. P. Jiang, N. Mizushima, LC3- and p62-based biochemical methods for the analysis of autophagy progression in mammalian cells. *Methods* **75**, 13–18 (2015).
3. R. Myerowitz, R. Puertollano, N. Raben, Impaired autophagy: The collateral damage of lysosomal storage disorders. *EBioMedicine* **63**, (2021).
4. H. Park, J. H. Kang, S. Lee, Autophagy in neurodegenerative diseases: A hunter for aggregates. *Int. J. Mol. Sci.* **21**, 3369 (2020).
5. R. Mathew, V. Karantza-Wadsworth, E. White, Role of autophagy in cancer. *Nat. Rev. Cancer* **7**, 961–967 (2007).
6. V. Kolluru, A. Tyagi, B. Chandrasekaran, M. Ankem, C. Damodaran, Induction of endoplasmic reticulum stress might be responsible for defective autophagy in cadmium-induced prostate carcinogenesis. *Toxicol. Appl. Pharmacol.* **373**, 62–68 (2019).
7. C. M. Neslund-Dudas, R. B. McBride, A. Kandegedara, B. A. Rybicki, O. N. Kryvenko, D. Chitale, N. Gupta, S. R. Williamson, C. G. Rogers, C. Cordon-Cardo, A. G. Rundle, A. M. Levin, Q. P. Dou, B. Mitra, Association between cadmium and androgen receptor protein expression differs in prostate tumors of African American and European American men. *J. Trace Elem. Med. Biol.* **48**, 233–238 (2018).
8. F. Nyqvist, I. Helmfrid, A. Augustsson, G. Wingren, Increased cancer incidence in the local population around metal-contaminated glassworks sites. *J. Occup. Environ. Med.* **59**, e84–e90 (2017).
9. A. C. McDonald, J. Gernand, N. R. Geyer, H. Wu, Y. Yang, M. Wang, Ambient air exposures to arsenic and cadmium and overall and prostate cancer-specific survival among prostate cancer cases in Pennsylvania, 2004 to 2014. *Cancer* **128**, 1832–1839 (2022).
10. V. Vijayakumar, M. R. Abern, J. S. Jagai, A. Kajdacsy-balla, Observational study of the association between air cadmium exposure and prostate cancer aggressiveness at diagnosis among a nationwide retrospective cohort of 230,540 patients in the united states. *Int. J. Environ. Res. Public Health* **18**, 8333 (2021).
11. J. Godt, F. Scheidig, C. Grosse-Siestrup, V. Esche, P. Brandenburg, A. Reich, D. A. Groneberg, The toxicity of cadmium and resulting Hazards for Human Health. *J. Occup. Med. Toxicol.* **1**, 22 (2006).
12. V. Rapisarda, E. Miozzi, C. Loreto, S. Matera, C. Fenga, R. Avola, C. Ledda, Cadmium exposure and prostate cancer: Insights, mechanisms and perspectives. *Front. Biosci. (Landmark Ed)* **23**, 1687–1700 (2018).
13. C. Kinsey, V. Balakrishnan, M. R. O'Dell, J. L. Huang, L. Newman, C. L. Whitney-Miller, A. F. Hezel, H. Land, PLAC8 links oncogenic mutations to regulation of autophagy and is critical to pancreatic cancer progression. *Cell Rep.* **7**, 1143–1155 (2014).
14. M. Mao, Y. Cheng, J. Yang, Y. Chen, L. Xu, X. Zhang, Z. Li, C. Chen, S. Ju, J. Zhou, L. Wang, Multifaced roles of PLAC8 in cancer. *Biomark. Res.* **9**, 73 (2021).
15. V. Kolluru, D. Pal, A. M. S. Papu John, M. K. Ankem, J. H. Freedman, C. Damodaran, Induction of Plac8 promotes pro-survival function of autophagy in cadmium-induced prostate carcinogenesis. *Cancer Lett.* **408**, 121–129 (2017).
16. S. Guzel, L. Kiziler, B. Aydemir, B. Alici, S. Ataus, A. Aksu, H. Durak, Association of Pb, Cd, and Se concentrations and oxidative damage-related markers in different grades of prostate carcinoma. *Biol. Trace Elem. Res.* **145**, 23–32 (2012).
17. C. Neslund-Dudas, A. Kandegedara, O. N. Kryvenko, N. Gupta, C. Rogers, B. A. Rybicki, Q. P. Dou, B. Mitra, Prostate tissue metal levels and prostate cancer recurrence in smokers. *Biol. Trace Elem. Res.* **157**, 107–112 (2014).
18. M. Karin, NF-κB as a critical link between inflammation and cancer. *Cold Spring Harb. Perspect. Biol.* **1**, a000141 (2009).
19. C. C. Huang, M. H. Shen, S. K. Chen, S. H. Yang, C. Y. Liu, J. W. Guo, K. W. Chang, C. J. Huang, Gut butyrate-producing organisms correlate to Placenta Specific 8 protein: Importance to colorectal cancer progression. *J. Adv. Res.* **22**, 7–20 (2020).
20. M. Mao, Y. Chen, Y. Jia, J. Yang, Q. Wei, Z. Li, L. Chen, C. Chen, L. Wang, PLCA8 suppresses breast cancer apoptosis by activating the PI3k/AKT/NF-κB pathway. *J. Cell Mol. Med.* **23**, 6930–6941 (2019).
21. P. Y. Ke, Molecular mechanism of Autophagosome-Lysosome fusion in mammalian cells. *Cells* **13**, 500 (2024).
22. A. K. Mankan, M. W. Lawless, S. G. Gray, D. Kelleher, R. McManus, NF-κB regulation: The nuclear response. *J. Cell Mol. Med.* **13**, 631–643 (2009).
23. B. Tyagi, B. Chandrasekaran, A. Tyagi, V. Shukla, U. Saran, N. Tyagi, S. Talluri, A. D. Juneau, H. Fu, M. K. Ankem, C. Damodaran, Exposure of environmental trace elements in prostate cancer patients: A multiple metal analysis. *Toxicol. Appl. Pharmacol.* **479**, 116728 (2023).
24. M. P. Waalkes, S. Rehm, Cadmium and prostate cancer. *J. Toxicol. Environ. Health* **43**, 251–269 (1994).
25. M. P. Waalkes, S. Rehm, M. G. Cherian, Repeated cadmium exposures enhance the malignant progression of ensuing tumors in rats. *Toxicol. Sci.* **54**, 110–120 (2000).
26. S. M. Alvarez, N. N. Gómez, L. Scardapane, M. W. Fornés, M. S. Giménez, Effects of chronic exposure to cadmium on prostate lipids and morphology. *Biometals* **20**, 727–741 (2007).
27. P. Aimola, M. Carmignani, A. R. Volpe, A. Di Benedetto, L. Claudio, M. P. Waalkes, A. van Bokhoven, E. J. Tokar, P. P. Claudio, Cadmium induces p53-dependent apoptosis in human prostate epithelial cells. *PLOS ONE* **7**, e33647 (2012).
28. W. E. Achanzar, B. A. Diwan, J. Liu, S. T. Quader, M. M. Webber, M. P. Waalkes, Cadmium-induced malignant transformation of human prostate epithelial cells. *Cancer Res.* **61**, 455–458 (2001).
29. K. Nakamura, Y. Yasunaga, D. Ko, L. L. Xu, J. W. Moul, D. M. Peehl, S. Srivastava, J. S. Rhim, Cadmium-induced neoplastic transformation of human prostate epithelial cells. *Int. J. Oncol.* **20**, 543–547 (2002).
30. W. Qu, H. Ke, J. Pi, D. Broderick, J. E. French, M. M. Webber, M. P. Waalkes, Acquisition of apoptotic resistance in cadmium-transformed human prostate epithelial cells: Bcl-2 overexpression blocks the activation of JNK signal transduction pathway. *Environ. Health Perspect.* **115**, 1094–1100 (2007).
31. W. E. Achanzar, M. M. Webber, M. P. Waalkes, Altered apoptotic gene expression and acquired apoptotic resistance in cadmium-transformed human prostate epithelial cells. *Prostate* **52**, 236–244 (2002).
32. W. E. Achanzar, K. B. Achanzar, J. G. Lewis, M. M. Webber, M. P. Waalkes, Cadmium induces c-myc, p53, and c-jun expression in normal human prostate epithelial cells as a prelude to apoptosis. *Toxicol. Appl. Pharmacol.* **164**, 291–300 (2000).
33. A. Eisenberg-Lerner, S. Bialik, H. U. Simon, A. Kimchi, Life and death partners: Apoptosis, autophagy and the cross-talk between them. *Cell Death Differ.* **16**, 966–975 (2009).
34. S. Jäger, C. Bucci, I. Tanida, T. Ueno, E. Kominami, P. Saftig, E. L. Eskelinen, Role for Rab7 in maturation of late autophagic vacuoles. *J. Cell Sci.* **117**, 4837–4848 (2004).
35. S. Segawa, Y. Kondo, Y. Nakai, A. Iizuka, S. Kaneko, M. Yokosawa, K. Furuyama, H. Tsuboi, D. Goto, I. Matsumoto, T. Sumida, Placenta specific 8 suppresses IL-18 production through regulation of autophagy and is associated with adult still disease. *J. Immunol.* **201**, 3534–3545 (2018).
36. M. Nivon, E. Richet, P. Codogno, A. P. Arrigo, C. Kretz-Remy, Autophagy activation by NFκB is essential for cell survival after heat shock. *Autophagy* **5**, 766–783 (2009).
37. A. Trocoli, M. Djavaheri-Mergny, The complex interplay between autophagy and NF-κB signaling pathways in cancer cells. *Am. J. Cancer Res.* **1**, 629–649 (2011).

38. S. de Carné Trécesson, F. Souazé, A. Basseville, A.-C. Bernard, J. Pécot, J. Lopez, M. Bessou, K. A. Sarosiek, A. Letai, S. Barillé-Nion, I. Valo, O. Coqueret, C. Guette, M. Campone, F. Gautier, P. P. Juin, BCL-X_L directly modulates RAS signalling to favour cancer cell stemness. *Nat. Commun.* **8**, 1123 (2017).
39. C. Chen, L. C. Edelstein, C. Gélinas, The Rel/NF-κB family directly activates expression of the apoptosis inhibitor Bcl-x_L. *Mol. Cell Biol.* **20**, 2687–2695 (2000).
40. L. He, G. A. Perkins, A. T. Poblenz, J. B. Harris, M. Hung, M. H. Ellisman, D. A. Fox, Bcl-xL overexpression blocks bax-mediated mitochondrial contact site formation and apoptosis in rod photoreceptors of lead-exposed mice. *Proc. Natl. Acad. Sci. U.S.A.* **100**, 1022–1027 (2003).
41. S. V. S. Rana, Metals and apoptosis: Recent developments. *J. Trace Elem. Med. Biol.* **22**, 262–284 (2008).
42. M. Jimenez-Preitner, X. Berney, M. Uldry, A. Vitali, S. Cinti, J. G. Ledford, B. Thorens, Plac8 is an inducer of C/EBPβ required for brown fat differentiation, thermoregulation, and control of body weight. *Cell Metab.* **14**, 658–670 (2011).
43. S. K. Connors, R. Balusu, C. N. Kundu, A. S. Jaiswal, C. G. Gairola, S. Narayan, C/EBPbeta-mediated transcriptional regulation of bcl-xl gene expression in human breast epithelial cells in response to cigarette smoke condensate. *Oncogene* **28**, 921–932 (2009).
44. Y. Yan, J. Liu, A. Lawrence, M. J. Dykstra, R. Fannin, K. Gerrish, C. J. Tucker, E. Scappini, D. Dixon, Prolonged cadmium exposure alters benign uterine fibroid cell behavior, extracellular matrix components, and TGFB signaling. *FASEB J.* **35**, e21738 (2021).
45. B. Chandrasekaran, A. Tyagi, U. Saran, V. Kolluru, B. V. Baby, V. R. Chirasani, N. V. Dokholyan, J. M. Lin, A. Singh, A. K. Sharma, M. K. Ankem, C. Damodaran, Urolithin A analog inhibits castration-resistant prostate cancer by targeting the androgen receptor and its variant, androgen receptor-variant 7. *Front. Pharmacol.* **14**, 1137783 (2023).
46. S. Bolte, F. P. Cordelières, A guided tour into subcellular colocalization analysis in light microscopy. *J. Microsc.* **224**, 213–232 (2006).
47. E. S. REYNOLDS, The use of lead citrate at high pH as an electron-opaque stain in electron microscopy. *J. Cell Biol.* **17**, 208–212 (1963).
48. J. Schindelin, I. Arganda-Carreras, E. Frise, V. Kaynig, M. Longair, T. Pietzsch, S. Preibisch, C. Rueden, S. Saalfeld, B. Schmid, J.-Y. Tinevez, D. J. White, V. Hartenstein, K. Eliceiri, P. Tomancak, A. Cardona, Fiji: An open-source platform for biological-image analysis. *Nat. Methods* **9**, 676–682 (2012).
49. J. Lam, P. Katti, M. Biete, M. Mungai, S. A. Shareef, K. Neikirk, E. G. Lopez, Z. Vue, T. A. Christensen, H. K. Beasley, T. A. Rodman, S. A. Murray, J. L. Salisbury, B. Glancy, J. Shao, R. O. Pereira, E. D. Abel, A. Hinton Jr., A universal approach to analyzing transmission electron microscopy with ImageJ. *Cells* **10**, 2177 (2021).
50. M. Jung, H. Choi, J. Y. Mun, The autophagy research in electron microscopy. *Appl. Microsc.* **49**, 11 (2019).
51. J. W. Kwon, H. K. Kwon, H. J. Shin, Y. M. Choi, M. A. Anwar, S. Choi, Activating transcription factor 3 represses inflammatory responses by binding to the p65 subunit of NF-κB. *Sci. Rep.* **5**, 14470 (2015).
52. G. Landini, G. Martinelli, F. Piccinini, Colour deconvolution: Stain unmixing in histological imaging. *Bioinformatics* **37**, 1485–1487 (2021).
53. A. Dobin, C. A. Davis, F. Schlesinger, J. Drenkow, C. Zaleski, S. Jha, P. Batut, M. Chaisson, T. R. Gingeras, STAR: Ultrafast universal RNA-seq aligner. *Bioinformatics* **29**, 15–21 (2013).
54. L. Wang, S. Wang, W. Li, RSeQC: Quality control of RNA-seq experiments. *Bioinformatics* **28**, 2184–2185 (2012).
55. S. Anders, W. Huber, Differential expression analysis for sequence count data. *Genome Biol.* **11**, R106 (2010).
56. I. de Bruijn, R. Kundra, B. Mastrogiacomo, T. N. Tran, L. Sikina, T. Mazor, X. Li, A. Ochoa, G. Zhao, B. Lai, A. Abeshouse, D. Baiceanu, E. Ciftci, U. Dogrusoz, A. Dufilie, Z. Erkoc, E. G. Lara, Z. Fu, B. Gross, C. Haynes, A. Heath, D. Higgins, P. Jagannathan, K. Kalletla, P. Kumari, J. Lindsay, A. Lisman, B. Leenknegt, P. Lukasse, D. Madela, R. Madupuri, P. van Nierop, O. Plantalech, J. Quach, A. C. Resnick, S. Y. A. Rodenburg, B. A. Satravada, F. Schaeffer, R. Sheridan, J. Singh, R. Sirohi, S. O. Sumer, S. van Hagen, A. Wang, M. Wilson, H. Zhang, K. Zhu, N. Rusk, S. Brown, J. A. Lavery, K. S. Panageas, J. E. Rudolph, M. L. Le Noue-Newton, J. L. Warner, X. Guo, H. Hunter-Zinck, T. V. Yu, S. Pilai, C. Nichols, S. M. Gardos, J. Philip, AACR Project GENIE BPC Core Team, AACR Project GENIE Consortium, K. L. Kehl, G. J. Riely, D. Schrag, J. Lee, M. V. Fiandalo, S. M. Sweeney, T. J. Pugh, C. Sander, E. Cerami, J. Gao, N. Schultz, Analysis and visualization of longitudinal genomic and clinical data from the AACR project GENIE biopharma collaborative in cBioPortal. *Cancer Res.* **83**, 3861–3867 (2023).
57. G. Tang, X. Liu, M. Cho, Y. Li, D. H. Tran, X. Wang, Pan-cancer discovery of somatic mutations from RNA sequencing data. *Commun. Biol.* **7**, 619 (2024).
58. A. Subramanian, P. Tamayo, V. K. Mootha, S. Mukherjee, B. L. Ebert, M. A. Gillette, A. Paulovich, S. L. Pomeroy, T. R. Golub, E. S. Lander, J. P. Mesirov, Gene set enrichment analysis: A knowledge-based approach for interpreting genome-wide expression profiles. *Proc. Natl. Acad. Sci. U.S.A.* **102**, 15545–15550 (2005).
59. D. Tang, M. Chen, X. Huang, G. Zhang, L. Zeng, G. Zhang, S. Wu, Y. Wang, SRplot: A free online platform for data visualization and graphing. *PLOS ONE* **18**, e0294236 (2023).

Acknowledgments: We acknowledge the assistance of the Joint Microscopy Laboratory (Luminosa confocal microscope) in the Texas A&M University School of Medicine and the National Institutes of Health (NIH) funding for the Luminosa confocal microscope (S10 OD032208). **Funding:** This research was supported by grants from the National Institute of Environmental Health Sciences (NIEHS), specifically R01ES028102 and R01ES030019, awarded to C.D. **Author contributions:** Conceptualization: C.D., M.K.A., and B.C. Methodology: C.D., V.S., A.T., B.C., and V.K. Investigation: V.S., A.T., B.C., B.T., B.S., V.K., and T.N.D. Validation: V.S., A.T., and B.C. Formal analysis: V.S., A.T., and B.C. Visualization: V.S., A.T., and B.C. Supervision: C.D. and M.K.A. Data curation: V.S., A.T., B.C., and B.T. Writing—original draft: V.S. and A.T. Writing—review and editing: C.D., M.K.A., A.T., and B.C. Resources: C.D. and M.K.A. Funding acquisition: C.D. Project administration: C.D. and M.K.A. **Competing interests:** The authors declare that they have no competing interests. **Data and materials availability:** All data needed to evaluate the conclusions in the paper are present in the paper and/or the Supplementary Materials.

Submitted 10 January 2025
Accepted 9 May 2025
Published 13 June 2025
10.1126/sciadv.adv8640